

## Topical Review

# Nonlinear coherent structures in granular crystals

C Chong<sup>1</sup>, Mason A Porter<sup>2,3,4</sup>, P G Kevrekidis<sup>5</sup> and C Daraio<sup>6</sup><sup>1</sup> Department of Mathematics, Bowdoin College, Brunswick, Maine 04011, United States of America<sup>2</sup> Department of Mathematics, University of California, Los Angeles, CA 90095, United States of America<sup>3</sup> Oxford Centre for Industrial and Applied Mathematics, Mathematical Institute, University of Oxford, Oxford OX2 6GG, United Kingdom<sup>4</sup> CABDyN Complexity Centre, University of Oxford, Oxford OX1 1HP, United Kingdom<sup>5</sup> Department of Mathematics and Statistics, University of Massachusetts, Amherst, Massachusetts 01003-4515, United States of America<sup>6</sup> Division of Engineering and Applied Science, California Institute of Technology, Pasadena, CA 91125, United States of AmericaE-mail: [cchong@bowdoin.edu](mailto:cchong@bowdoin.edu)

Received 30 March 2016, revised 18 April 2017

Accepted for publication 1 June 2017

Published 6 September 2017

**Abstract**

The study of granular crystals, which are nonlinear metamaterials that consist of closely packed arrays of particles that interact elastically, is a vibrant area of research that combines ideas from disciplines such as materials science, nonlinear dynamics, and condensed-matter physics. Granular crystals exploit geometrical nonlinearities in their constitutive microstructure to produce properties (such as tunability and energy localization) that are not conventional to engineering materials and linear devices. In this topical review, we focus on recent experimental, computational, and theoretical results on nonlinear coherent structures in granular crystals. Such structures—which include traveling solitary waves, dispersive shock waves, and discrete breathers—have fascinating dynamics, including a diversity of both transient features and robust, long-lived patterns that emerge from broad classes of initial data. In our review, we primarily discuss phenomena in one-dimensional crystals, as most research to date has focused on such scenarios, but we also present some extensions to two-dimensional settings. Throughout the review, we highlight open problems and discuss a variety of potential engineering applications that arise from the rich dynamic response of granular crystals.

Keywords: granular crystals, nonlinear waves, breathers, nonlinear dynamics, traveling waves, dispersive shock waves

(Some figures may appear in colour only in the online journal)

**1. Introduction**

Granular crystals consist of closely packed arrays of particles that traditionally are modeled as interacting with each other elastically<sup>7</sup> [146, 163, 176, 189] (see figure 1). The simplest description of a granular crystal, which one can construe as

a type of metamaterial, models only forces that result from the contact of adjacent particles. The exact nature of this contact force depends on the geometry of the particles in contact, the contact angle, and elastic properties of the particles [100]. Consequently, by changing the material properties or shapes of the particles, one can modify the effective stiffness of a granular crystal. One can also apply an initial prestress (i.e. a precompression) by applying a static force

<sup>7</sup> See section 3 for a brief discussion of more general types of interactions.

at the boundaries of the crystal. This controls the strength of the system's nonlinearity, which can range from almost linear (for strong precompression) to purely nonlinear (no precompression). The remarkable tunability of granular crystal stems both from this ability to tune the response from a weakly nonlinear regime to a strongly nonlinear regime and from the ability to study crystals with either homogeneous or controllably heterogeneous configurations (e.g. periodic arrangements, settings with defects, random arrangements, and so on). This flexibility makes granular crystals potentially useful for a host of applications, including shock- and energy-absorbing layers [45, 50, 64, 85], actuating devices [107], acoustic lenses [181], acoustic diodes [19] and switches [124], sound scramblers [46, 147], and more.

Granular crystals are also an ideal test bed for fundamental studies of nonlinear dynamics, as they constitute a prototypical (and experimentally convenient) realization of a classical system of nonlinearly coupled oscillators. The simplest and most standard type of granular crystal consists of a one-dimensional (1D) crystal with spherical particles. One can envision these spheres as particles that are coupled by nonlinear springs and do not have any on-site forces. We use the term 'granular chain' to refer to an array of particles aligned in a 1D configuration. More generally, the term 'granular crystals' includes such chains as examples but can also indicate more general configurations. The broad range of interest in granular chains (and in granular crystals more generally) is apparent in the diverse nature of the publications about them; these range from predominantly experimental investigations that focus on applications to theoretical studies that concentrate on rigorous mathematical proofs. V. F. Nesterenko is largely responsible for bringing significant attention to the subject of granular crystals, and his influential 2001 book [146] is a canonical starting point for researchers who are interested in this subject. Since the publication of Nesterenko's book, there has been a burst of activity on granular crystals. These activities were discussed in a 2008 review article by Sen *et al* [176], and specific areas in the study of granular crystals have been surveyed in specialized reviews that were published as book chapters [189, 198]. There is also a very recent popular article in the magazine *Physics Today* [163]. Our review complements [176, 189, 198] and highlights a wealth of exciting research on granular crystals that has appeared in the last decade<sup>8</sup>.

The explosion of recent results in granular crystals has resulted from the emergence of numerous research groups with the ability to perform detailed quantitative monitoring of granular crystals by using novel techniques (including non-invasive ones, such as photography [217] or laser Doppler vibrometry [26, 125]). These exciting advances have ushered the investigation of granular crystals into a new era of theory, computation, and experiments [163] that we will explore in the present paper. In this topical review, we emphasize nonlinear coherent structures, such as traveling solitary waves, dispersive shock waves, and discrete breathers.

<sup>8</sup> We also note that although other types of granular systems—such as soils, sand, and cereals—also have rich and diverse dynamics, their physical properties are rather different from those of granular crystals. They are beyond the scope of our article, but interested readers can examine the reviews [16, 128].

The remainder of our topical review is structured as follows. We present experimental setups in section 2, discuss model equations in section 3, and examine the linear regime and dispersion in section 4. We then discuss traveling solitary waves in section 5, dispersive shock waves in section 6, and breathers in section 7. We give an introduction to two-dimensional granular crystals in section 8, and we conclude in section 9. We highlight open questions and possible applications of granular crystals throughout the article.

## 2. Experimental setups

Most experimental studies on the dynamic response of granular crystals have focused on the elastic response of 1D and two-dimensional (2D) macroscale systems, which are usually composed of 10–800 particles, with diameters in the millimeter-to-centimeter range. Most granular crystals use spherical particles, although an increasing number of recent studies have examined other geometries, including ellipsoidal particles [148], cylindrical particles [108, 112], and a combination of different particle shapes [119]. Researchers have used particles made of various materials [146, 176, 189]. The most commonly used constitutive materials are stainless steel ball bearings [146], although other metals (e.g. aluminum, brass, and bronze) [20, 39, 40] and softer particles—composed of polymeric materials such as Homalite [178], nylon [40], Teflon (PTFE) [46], and Delrin [118]—have also been employed.

Experimental techniques for monitoring coherent structures (such as propagating waves) in granular crystals (see figures 1(a) and (b)) often entail assembling particles inside cylindrical [147] or square support guides [39], support rods [20], or tracks [97]. In these systems, one can create an initial excitation of propagating waves using drop-weight impacts of striker particles [147], electromagnetic actuators [39], piezo-electric transducers [49], or noncontact laser ablation [203]. Typical initial excitations of granular chains include single impulses, shocks, and continuous harmonic vibrations. Much of the same experimental approaches used in 1D granular chains have also been employed to study nonlinear wave propagation in elastic 2D [118, 121] and three-dimensional (3D) granular crystals with Hertzian contacts [10].

There are a variety of ways to detect coherent structures in granular crystals. The most common approach of a local measurement of transient force profiles in selected particles relies either on using piezo-electric transducers embedded at a boundary and/or inside the particles [46, 98] or on using triaxial accelerometers [121]. The use of embedded sensors allows accurate detection of force profiles, but it is limited to a small number of locations in a granular crystal. Additionally, embedded sensors can be intrusive to the dynamics from (i) an impedance mismatch between the piezoelectric layer and the particle materials and (ii) the presence of wires, which are needed to transfer the recorded signal. Less intrusive techniques include using laser vibrometers [26, 125], which can measure the displacement and velocity of selected particles. This approach has the advantage of being able to scope individual particles at will, leading to the potential to visualize the entire spatiotemporal dynamics of a granular crystal. Optical techniques, such

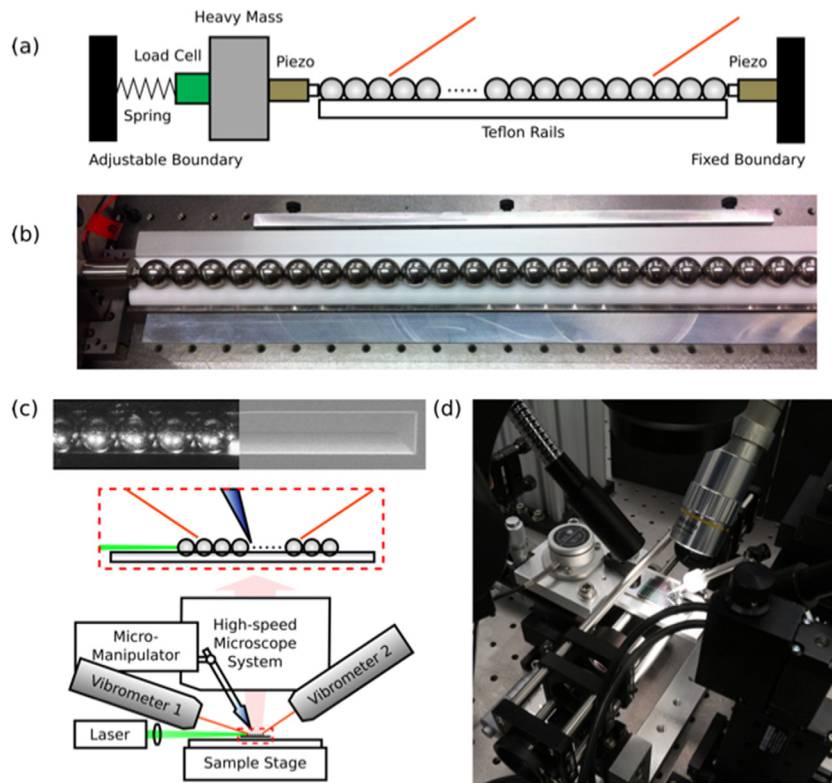


**Figure 1.** Macroscale and microscale experimental setups for granular chains. (a) Schematic diagram of a typical macroscale setup that includes support rods, boundaries, excitation capabilities, and a detection system. (The orange lines represent laser interferometers, which monitor the displacement and velocity of selected particles.) (b) Laboratory realization of the setup in panel (a) with particles whose diameter is about 1.9 cm. (c) Image and schematic diagram of a typical microscale setup that includes support grooves, robotic manipulation, and optical excitation and detection capabilities. The inset shows an optical image of a granular chain composed of stainless steel particles (of roughly 300 microns in diameter) and a scanning-electron-microscopy image of the support grooves. (d) Laboratory realization of the setup in (c). Panels (a) and (b) used with permission from Paul Anzel. Panels (c) and (d) reprinted figure with permission from [126], Copyright (2016) by the American Physical Society.

as photoelasticity, have also enabled full-field visualization of coherent structures in 1D and 2D systems, although such approaches are limited to crystals composed of relatively soft particles and to disk-shaped elements (cylinders that are relatively small along the principle axis) [74, 217]. Additionally, carbon paper has been employed to measure transmitted force at the edge of 3D particle lattices [142].

Experimental methods to study 1D granular crystals (i.e. granular chains) are now well-established. One of the challenges facing experimentalists today is the ability to create granular crystals in higher dimensions (in 2D and even 3D), where it is necessary to use a larger number of particles than in 1D. Increasing the number of particles in a densely packed crystal translates to increasing the amount of connectivity between particles. This demands high precision in particle fabrication (in particular, in their sphericity and in their surface finish and asperities), and small tolerances in crystal assembly (which, for the most part, have been arranged manually to date), both of which are difficult to achieve. Experimental systems with a very large number of particles are also more sensitive to the presence of defects (e.g. gaps between contacts or misalignment) and disorder, and such configurations are therefore less reproducible than systems with fewer particles [120].

An exciting experimental direction in granular crystals is to explore the dynamics of systems that are composed of

‘engineered’ particles. For example, heavy particles with a soft coating [44] have an exceptionally low signal speed, and particles with internal [21] or external resonant masses [72] allow the formation of tunable and low-frequency band gaps in transmission spectra.

The experimental platforms that have been developed for granular crystals have yielded fundamental proof-of-principle demonstrations of nonlinear phenomena predicted by computational and analytical studies. However, most of the experiments are limited to the study of crystals with contact interactions in the elastic regime. Deviations from a purely elastic regime have been identified in the presence of dissipation [29, 149, 166], which arises in experiments either from (1) the presence of friction between particles and supports or from (2) intrinsic losses in the particles (e.g. vibrational modes and viscoelasticity). Recent experimental approaches that deviate from linear elasticity have been helpful for characterizing granular crystals with elasto-plastic contacts [24–26]. The effects of plasticity around a contact between particles is an important factor for using granular crystals as impact-protecting layers. Experimental setups to study impulse mitigation and redirection in elasto-plastic granular crystals excited by high-velocity impactors have included modified split-Hopkinson bar systems [24, 154, 155] and spring-loaded coils [25].

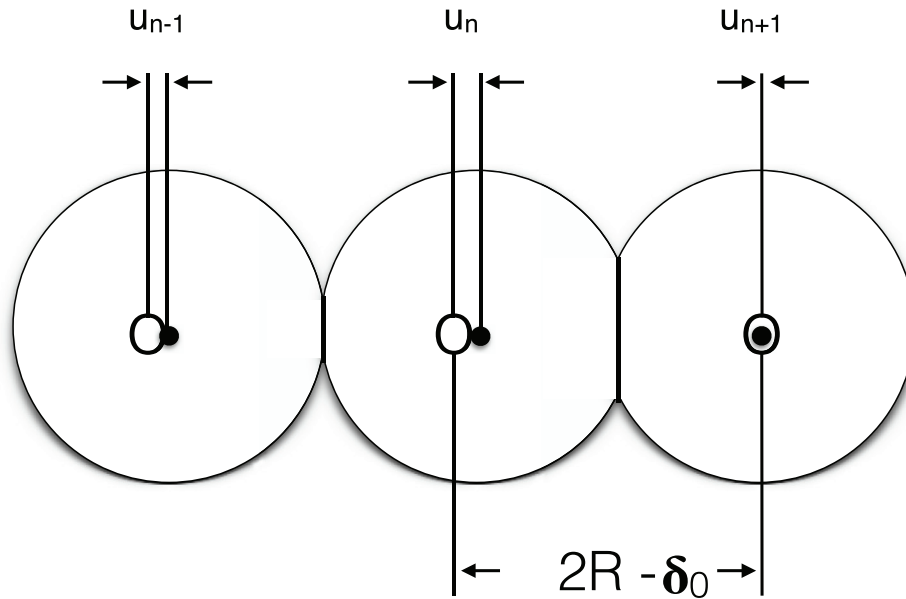


**Figure 2.** One-dimensional monomer granular chain compressed by a static force  $F_0$ . The open circles represent the initial positions of the particle centers in static equilibrium, and the black circles indicate the displaced positions. [146] 2001 © Springer-Verlag New York. With permission of Springer.

The studies that we mentioned above concern macroscale particles (with millimeter-sized to centimeter-sized diameters). The solitary waves supported by nonlinear granular chains have a spatial wavelength of roughly five particle diameters (although the situation is more subtle than this, as we will discuss in sections 5.1 and 5.2) and a propagation speed that is proportional to their amplitude. These spatial and temporal properties translate to signals that travel through macroscale granular chains with frequencies in the 1–100 kHz range. Using strongly nonlinear signals in acoustic imaging or in non-destructive evaluation requires acoustic excitations in the ultrasonic regime (i.e. microscopic particle sizes). Recent numerical investigations have examined coherent structures in smaller-scale granular crystals (e.g. nanoscale buckyball particle chains [205]), but much remains unknown about the propagation of dynamic excitations through chains of micrometer-size particles in contact (and more generally about coherent structures in such granular crystals). Although one expects the fundamental elasticity of the contacts to remain valid when particles have diameters of about 1–100 micrometers, the dynamics of micro-particle chains are not simply scaled-down version of their macroscale counterparts. One expects microscale granular crystals to exhibit qualitatively different dynamics, which are affected by the presence of adhesive forces, viscous drag, electrostatic charges, surface asperities, and a greater sensitivity to disorder. Because of these effects, experimental studies at these scales are challenging: they require high accuracy in particle packing, excitation, and detection of waves with non-contact techniques (see the next paragraph), which are nonintrusive and more precise than those that are used for macroscale systems.

Recent studies of 1-micrometer-diameter silica spheres employed a laser-induced transient grating technique to excite surface acoustic waves and measure their dispersion [18]. However, this technique is not suitable for capturing nonlinear, transient wave phenomena, such as those found in macroscale systems. At slightly larger scales, chains of steel particles with

diameters of about 2–300 micrometers have been investigated using non-contact optical techniques [126]. In these experiments, particles were aligned in microfabricated grooves using a robotic positioning systems, and high-speed microscopy imaging was used to ensure high positioning accuracy (see figures 1(c) and (d)).

### 3. Model equations

The force that results from the deformation of two spherical particles in contact is described by the classical Hertz law

$$F(x) = A[x]_+^{3/2}, \tag{1}$$

where  $x$  is the overlap between the two particles and  $A$  is the material parameter (see also equation (4) below). A Hertzian interaction between a pair of particles occurs only when they are in contact, so each particle is affected directly only by its nearest neighbors and experiences a force from a neighbor only when it overlaps with it. This yields the bracket

$$[x]_+ = \begin{cases} x, & \text{if } x > 0 \\ 0, & \text{if } x \leq 0 \end{cases} \tag{2}$$

in equation (1). The original derivation of the contact law (1) is in Hertz’s seminal work [83], and [100] has a more modern version of it. The full derivation described in [83, 100] is somewhat cumbersome, and Sen *et al* gave a brief ‘back-of-the-envelope’ derivation of it in [176]. The nonlinearity exponent  $p$  depends on the geometry of the contact between particles. For example,  $p = 3/2$  for spherical particles. Cylindrical particles whose axes lie in the same plane but are not parallel also have an exponent of  $p = 3/2$ . In this case, the material parameter  $A$  depends on axis orientation. Other particle geometries can lead to exponents other than  $3/2$ . For example, hollow spheres have interaction laws that vary as a function of shell thickness [100].

Assuming that the only relevant force arises from elastic contact between particles (see figure 2 for an illustration), the 1D equations of motion for a finite-length granular chain (i.e. a 1D granular crystal) are

$$\ddot{u}_n = \frac{A_n}{m_n} [\delta_{0,n} + u_{n-1} - u_n]_+^p - \frac{A_{n+1}}{m_n} [\delta_{0,n+1} + u_n - u_{n+1}]_+^p, \quad (3)$$

where  $u_n$  is the displacement of the  $n$ th particle (with  $n \in \{1, 2, \dots, N\}$ , where  $N$  is the number of particles) measured from its equilibrium position in an initially compressed chain,  $m_n$  is the mass of the  $n$ th particle, and  $\delta_n = (F_0/A_n)^{1/p}$  is a static displacement for each particle that arises from the static load  $F_0 = \text{const.}$  (See figure 2 for an illustration.) For spherical particles, the exponent is  $p = 3/2$  and the parameter  $A_n$ , which reflects the material and the geometry of the chain's particles, has the form

$$A_n = \frac{4E_n E_{n+1} \sqrt{\frac{R_n R_{n+1}}{R_n + R_{n+1}}}}{3E_{n+1}(1 - \nu_n^2) + 3E_n(1 - \nu_{n+1}^2)}, \quad (4)$$

where  $E_n$  is the elastic (Young) modulus of the  $n$ th particle,  $\nu_n$  is its Poisson ratio, and  $R_n$  is its radius. Important special cases of equation (3) include monoatomic (i.e. ‘monomer’) chains (in which all particles are identical, so  $A_n = A$ ,  $m_n = m$ , and  $\delta_{0,n} = \delta_0$ ), period-2 diatomic chains, and chains with impurities (e.g. a ‘host’ monomer chain with a small number of ‘defect’ particles of a different type). The simplest type of period-2 diatomic chain (which is sometimes simply called a ‘dimer’ chain as a shorthand<sup>9</sup>) consists of alternating particles of two types, so  $A_n = A$ ,  $\delta_{0,n} = \delta_0$ , and the mass is  $m_n = m_0$  for even  $n$  and  $m_n = m_1$  for odd  $n$ . In such a chain, the mass ratio  $m_1/m_0$  is the only additional parameter other than those in the monomer case. We use the term ‘ $M$ -mer’ for period- $M$  chains with  $M > 2$ .

We now present some basic analytical considerations for the equations of motion (3). It is convenient to work in so-called ‘strain variables’  $y_n = u_{n+1} - u_n$ . For a monomer chain, equation (3) becomes

$$\ddot{y}_n = \frac{A}{m} (2[\delta_0 - y_n]_+^{3/2} - [\delta_0 - y_{n-1}]_+^{3/2} - [\delta_0 - y_{n+1}]_+^{3/2}). \quad (5)$$

Introducing the scaling  $t \rightarrow t \sqrt{\frac{A}{m}}$  allows us to write equation (5) as

$$\ddot{y}_n = (2[\delta_0 - y_n]_+^{3/2} - [\delta_0 - y_{n-1}]_+^{3/2} - [\delta_0 - y_{n+1}]_+^{3/2}). \quad (6)$$

If  $\delta_0 \neq 0$ , one can also normalize the precompression by rescaling the amplitude  $y_n$  [146]. For an infinite lattice (i.e.  $n \in \mathbb{Z}$ ), equation (3) has the Hamiltonian

$$H = \sum_{n \in \mathbb{Z}} \frac{1}{2} m_n \dot{u}_n^2 + V_n(u_{n+1} - u_n), \quad (7)$$

<sup>9</sup> Alternatively, one can use the term ‘dimer’ for any chain that consists of two types of particles but are not necessarily arranged with a spatial period of 2. In this article, a ‘dimer’ has a spatial period of 2, a ‘trimer’ has a spatial period of 3 (whether or not there are three distinct types of particles), and so on.

where the potential function is

$$V_n(y_n) = \frac{2}{5} A_{n+1} [\delta_{0,n} - y_n]_+^{5/2} + \phi_n, \quad \text{with} \\ \phi_n = -\frac{2}{5} A_{n+1} [\delta_{0,n}]^{5/2} + A_{n+1} [\delta_{0,n}]^{3/2} y_n. \quad (8)$$

Note that  $\phi_n$  in equation (8) implies that  $V'_n(0) = 0$  and  $V''_n(0) \geq 0$ , which is necessary to ensure that the classical ground state (for which  $u_n = \dot{u}_n = 0$ ) is a minimum of the energy  $H$  [69]. For the specific case of granular chains (with either zero or nonzero precompression), see [133]. The latter case is associated with  $V''_n(0) > 0$ , and the former is associated with  $V''(0) = 0$ .

Equation (3) is the simplest model for the description of a granular chain. It neglects many features, leading to disparities between its solutions and experimental observations. One potentially important feature is particle rotation [8, 27, 139], and another is that the contact points of particles cannot be aligned perfectly in experiments because of clearance between the particles and support rods [126]. This is likely to result in dynamic buckling of a granular chain when particles exhibit high-amplitude motion. In 1D settings, effects from the above two features are negligible in a variety of experimental configurations, but the role of rotation is considerably more important in higher-dimensional settings [42, 139, 207, 209, 211].

Additionally, as we explained above, the model of equation (3) is Hamiltonian in nature. This is a useful idealization for understanding the principal wave and coherent-structure phenomenology in granular chains, but realistic granular crystals have dissipative effects (e.g. from wave attenuation) that can significantly modify the coherent-structure dynamics from those predicted by a Hamiltonian description like equation (3). A customary approach is to incorporate a dashpot form of dissipation,  $F_d^{(1)} = -\dot{u}_n m_n / \tau_n$  (where  $\tau_n$  is a characteristic time scale), to describe experimental observations qualitatively (and, with parameter fitting, even quantitatively in some cases) [19, 87]. Another recent proposal [166, 167] is to explore a form of dissipation that involves a discrete Laplacian in the velocities<sup>10</sup>. The specific form employed for the force was  $F_d^{(2)} = m_n [(\dot{u}_{n-1} - \dot{u}_n) / \tau_{n-1,n} - (\dot{u}_n - \dot{u}_{n+1}) / \tau_{n,n+1}]$ , which was considered in the context of a monomer chain, and it was assumed that  $\tau_{n-1,n}$  is constant along the lattice. This approach was validated mathematically using perturbation methods in [23]. Subsequent generalizations of this functional form include power laws of the relative velocities [29] and more complicated forms, such as [199]

$$F_d^{(3)} \propto m_n (\sqrt{u_{n-1} - u_n} (\dot{u}_{n-1} - \dot{u}_n) - \sqrt{u_n - u_{n+1}} (\dot{u}_n - \dot{u}_{n+1})),$$

which is inspired by viscoelasticity theory and involves both displacements and velocities. Additionally, see [76] for an attempt to use finite-element modeling to derive a form for dissipative effects in granular crystals. However, despite the multitude of proposed models for incorporating dissipation, presently there is

<sup>10</sup> This idea is reminiscent of Navier–Stokes damping; see e.g. the discussion in [159] about the physical interest in such a functional form for the creation of ‘lattice turbulence’.

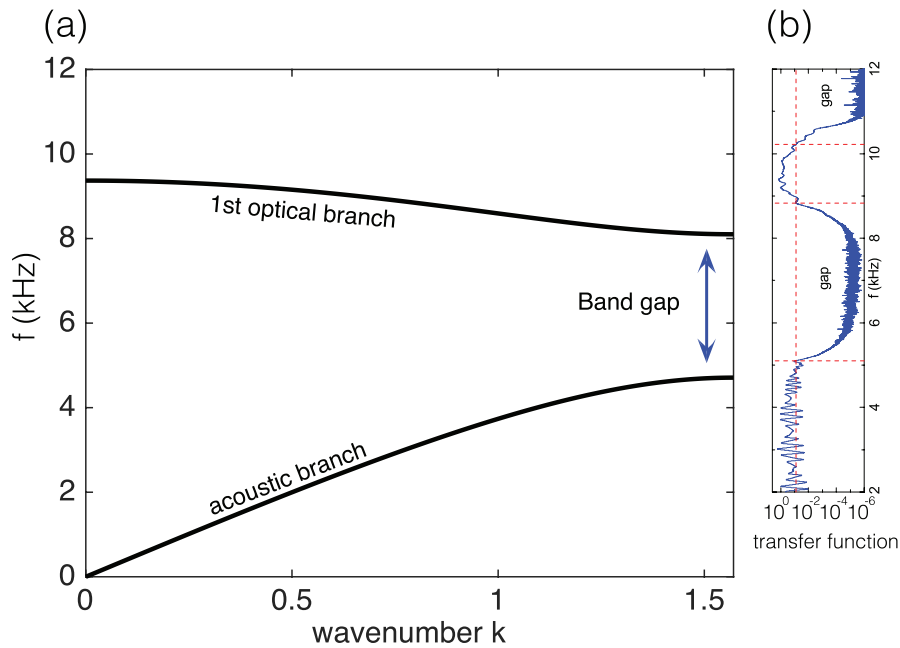


**Figure 3.** Pass bands (acoustic and optical) and band gap for the diatomic granular chain considered in [20]. (a) Analytical expression derived from the corresponding dispersion relations. (b) Experimental transfer function inferred when sending ‘white noise’ from one side through the system and then retrieving (on the other side) only the frequencies that belong to the pass bands (observe that the experimental and theoretical cutoff frequencies are somewhat different.) Reprinted figure with permission from [20], Copyright (2010) by the American Physical Society.

no universally accepted functional form to describe dissipative effects in granular crystals. Features such as plastic deformation [24–26, 154–156] and damping due to rotation may also account for some of the wave attenuation that has been observed in experiments [208]. The correct way to model such effects in granular crystals is an important open research problem. In the present review article, we mostly restrict our attention to Hamiltonian models of granular crystals (and especially equation (3)).

#### 4. Linear regime and dispersion

The nature of the equations of motion (3) is reminiscent of a Fermi–Pasta–Ulam (FPU) oscillator chain [48, 60, 71]. The connection is especially evident in the weakly nonlinear regime, in which the dynamic strains are small compared to the static precompression:

$$\frac{|u_n - u_{n+1}|}{\delta_{0,n}} \ll 1. \quad (9)$$

One can then Taylor expand the potential function to obtain

$$V'_n(y_n) \approx K_{2,n}y_n + K_{3,n}y_n^2 + K_{4,n}y_n^3, \quad (10)$$

where

$$\begin{aligned} K_{2,n} &= \frac{3}{2}A_{n+1}\delta_{0,n}^{1/2}, & K_{3,n} &= -A_{n+1}\frac{3}{8}\delta_{0,n}^{-1/2}, \\ K_{4,n} &= -A_{n+1}\frac{3}{48}\delta_{0,n}^{-3/2}. \end{aligned} \quad (11)$$

The function  $V_n(y)$  in equation (11) is the classical FPU potential (also called the ‘ $K_2$ – $K_3$ – $K_4$  potential’ or the ‘ $\alpha$ – $\beta$  potential’) [71]. The corresponding linear problem,

$$\ddot{u}_n = \frac{K_{2,n}}{m_n}(u_{n-1} - u_n) - \frac{K_{2,n+1}}{m_n}(u_n - u_{n+1}), \quad (12)$$

is a prototypical example of a coupled spring–mass system that serves as a textbook model for vibration modes [113]. For a monomer chain, equation (12) has plane wave solutions,

$$u_n(t) = e^{i(kn + \omega t)}, \quad k \in [0, \pi],$$

where the angular frequency  $\omega$  and the wavenumber  $k$  are related through the dispersion relation

$$[\omega(k)]^2 = \frac{4K_2}{m} \sin^2(k/2). \quad (13)$$

Equation (13) implies that the largest possible angular frequency of a plane wave is  $\omega_0 = 2\sqrt{K_2/m}$  (the so-called ‘cutoff point’). It thereby highlights the role of the lattice dynamical system (12) as a filter that allows the transmission of frequencies  $\omega < \omega_0$  but prohibits the transmission of frequencies  $\omega > \omega_0$ . The sound speed  $c_s$ , which indicates the maximum speed of a linear wave, is defined as the phase velocity  $\omega(k)/k$  in the limit  $k \rightarrow 0$ . In this case,  $c_s = \sqrt{K_2/m}$ . The single (positive) branch of the dispersion curve represented by equation (13) is called the ‘acoustic band’ of the linear spectrum. If the particles in a granular chain are arranged in a periodic manner with period  $M \in \mathbb{Z}^+$  (e.g.  $M = 2$  for a dimer), then the linear problem (12) is solved by Bloch waves

$$u_n(t) = f_n e^{i(kn + \omega t)}, \quad f_n = f_{n+M} \in \mathbb{C}, \quad k \in [0, \pi/M]. \quad (14)$$

One can compute the dispersion relation by solving the  $M \times M$  matrix eigenvalue problem obtained by substituting equations (14) into (12). This results in  $M$  eigenvector–eigenvalue pairs  $(\mathbf{f}, -\omega^2)$ , where  $\mathbf{f} = (f_1, f_2, \dots, f_M)^T$

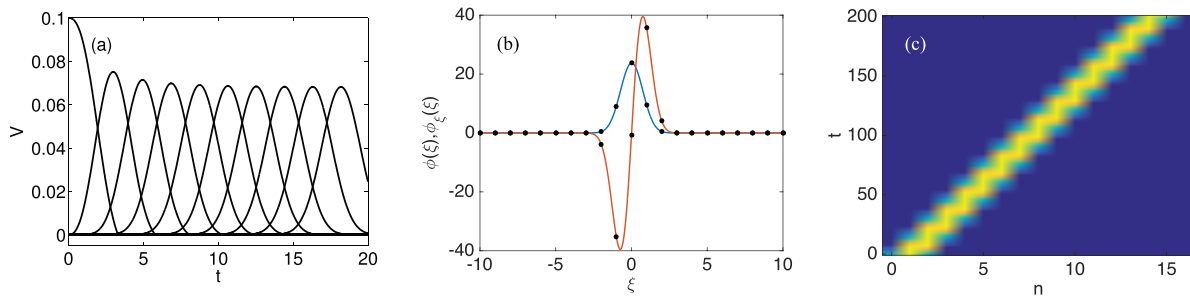


**Figure 4.** (a) For a monomer granular chain, a compression wave travels through the chain after it is struck at one end. After the wave has traveled a few lattice sites, it appears as though a constant shape profile forms and propagates through the chain. Each bell-shaped curve corresponds to the velocity profile of a single particle. (b) Solution of equation (18) (solid curves), which represents a genuine traveling solitary wave. The markers give the associated locations on the lattice. (c) Contour plot of the evolution of equation (3) with initial data given by the solitary wave in panel (b).

[113]. We use notation so that eigenvalues are ordered as  $-\omega_1^2(k) \geq -\omega_2^2(k) \geq \dots \geq -\omega_M^2(k)$ . The branch corresponding to  $-\omega_1^2(k)$  is called the ‘acoustic band’, and  $-\omega_j^2(k)$  is called the  $(j - 1)$ th ‘optical band’ (where  $j > 1$ ). See figure 3 for an example of a dispersion relation in a diatomic granular chain. If the chain has finite length or is not arranged in a periodic manner, one can obtain the angular frequencies of the linear modes (which are not necessarily sinusoidal in space) numerically by solving the  $N \times N$  eigenvalue problem that results by substituting the ansatz  $u_n(t) = \mathbf{v}e^{i\omega t}$ , with  $\mathbf{v} = (v_1, v_2, \dots, v_N)^T$ , into equation (12), where  $N$  is the length (i.e. number of particles) of the chain. In some special cases, one can approximate these eigenvalues analytically. For example, this is possible for a granular chain with a small number of impurities [134, 135]. See [99] for a relevant study for strongly nonlinear chains, and see [191] for a relevant study of weakly nonlinear chains. In a finite-length granular chain, the boundary conditions and length affect the mode shapes and introduce new modes, such as gap modes and edge modes (i.e. surface modes) [200].

Now that we have reviewed the dynamics of linear granular chains, we will discuss the effects of nonlinearity in the next several sections. As we will see, nonlinearity has a significant impact on the formation, propagation, and aggregate dynamics of waves and other coherent structures. In our discussions, it will nevertheless be helpful to keep the linear dynamics in mind.

## 5. Traveling solitary waves

### 5.1. Continuum modeling and the Nesterenko solitary wave

In 1985, Lazaradi and Nesterenko reported a new type of solitary wave [116] (see [213] for a review of solitary waves) that they found by striking one side of an uncompressed monomer granular chain with another particle. The resulting waveform was localized like a traditional solitary wave [214], but its tails exhibited much faster decay, and it was pondered whether the wave, a new type of solitary wave (see figure 4), might even have compact support [146]<sup>11</sup>. The experiments of Lazaradi and Nesterenko [116] were performed in the absence of static

precompression. In this case, equation (3) is purely nonlinear, and it is very challenging to study it analytically because the nonlinearity is not smooth (as the quantity  $V'''(0)$  is undefined in the absence of precompression). One of the first analytical results on a purely nonlinear granular chain was due to Nesterenko [145], who derived an explicitly solvable partial differential equation as an approximation to equation (3). This follows a standard procedure in discrete models by using a long-wavelength (i.e. near-continuum) limit in which one expects that the spatial extent of the wave is much longer than the spacing of the underlying lattice. A standard mechanism to transfer from the original discrete framework to this continuum limit is to introduce a small parameter  $\epsilon$  and define a new variable  $U(X, T) \approx u_n(t)$  that approximates a solution to equation (3), where the independent variables  $X$  and  $T$  generally depend on  $\epsilon$ . In the remainder of our article, we use the notation  $U(X, T)$  to represent a continuum approximation of the displacement  $u_n(t)$ , and we use  $Y(X, T)$  to represent a continuum approximation of the strain  $y_n(t)$ . We consider different scalings throughout the review, but we use the same notation for them for simplicity. In our first example, we define  $X = \epsilon n$  and  $T = \epsilon t$ . Differences become partial derivatives through a Taylor expansion of the new variable  $U$ . We thus write

$$U(\epsilon(n \pm 1), T) = U(X, T) \pm \partial_X U(X, T)\epsilon + \partial_X^2 U(X, T)\frac{\epsilon^2}{2} \pm \partial_X^3 U(X, T)\frac{\epsilon^3}{3!} + \partial_X^4 U(X, T)\frac{\epsilon^4}{4!} + \dots,$$

where  $\partial_X^j$  denotes the  $j$ th partial derivative with respect to the variable  $X$ . Because  $\epsilon$  is supposed to be small, the new variable  $U(X, T)$  has a wavelength that is large relative to that of the underlying lattice. Using the scaling  $X = \epsilon n, T = \epsilon t$ , one can derive a continuum model from equation (3) that is equivalent to the one that Nesterenko derived. One obtains

$$\partial_T^2 U = -\partial_X \left[ (-\partial_X U)^p + \frac{\epsilon^2}{12} \left( \partial_X^2 (-\partial_X U)^p - \frac{p(p-1)}{2} (-\partial_X U)^{p-2} \partial_X^2 U^2 \right) \right], \quad (15)$$

<sup>11</sup> A solitary wave with compact support is called a ‘compacton’ [170].

where we have assumed that the parameters are normalized (i.e.  $A = m = 1$ ). See [146, chapter 1.3] for the original derivation, and see [162] for a detailed version of the derivation for a dimer chain. The derivation of equation (15) assumes a long wavelength (i.e.  $\epsilon \rightarrow 0$ ), although traditionally  $\epsilon = 1$  has been used. Consequently, one can construe equation (15) with  $\epsilon = 1$  as a ‘quasicontinuum’ model, as it does not possess a small parameter, so it is not a self-consistent asymptotic procedure. This is one of the limitations of equation (15), as we will discuss in section 5.3. For now, let’s press on with equation (15) despite its limitations and seek traveling wave solutions. We define the coordinate  $\xi = X - cT$  and the new strain variable  $r(\xi) = U_\xi(\xi)$ . Substituting the traveling wave ansatz  $r(\xi)$  into equation (15) leads to an ordinary differentially equation (ODE) that can be solved explicitly [146, chapter 1.3]. Among the solutions of this ODE, one of particular interest is (what has come to be known as) the ‘Nesterenko solitary-wave solution’ (which is also sometimes called the ‘Nesterenko soliton’ or ‘Nesterenko compacton’) [7, 146]:

$$r(\xi) = \begin{cases} \left( \frac{2}{1+p} \right)^{\frac{1}{1-p}} |c|^{\frac{2}{p-1}} \cos^{\frac{2}{p-1}} \left( \xi \sqrt{6 \frac{(p-1)^2}{p(p+1)}} \right), & |\xi| < \pi \sqrt{\frac{p(p+1)}{24(p-1)^2}}, \\ 0, & \text{otherwise.} \end{cases} \quad (16)$$

This solution agrees reasonably well with direct numerical computations of solitary waves of equation (3) [145]. Note that if one starts with the strain-variable formulation in equation (6) and performs the same derivation for a new continuum approximation  $Y(X, T)$ , then  $Y(\xi) \neq r(\xi)$ . See the derivation and discussion in [7].

In the approximation (16), the amplitude of the wave scales with its speed  $c$  (a nonlinear analog of a dispersion relation) and the wave has a nonzero value only for a finite number of lattice sites (roughly 5 particles for a Hertzian interaction). Specifically, this suggests that the wave is *genuinely* compact and thus takes the form of a compacton. However, as we show in section 5.2, this is not the case, although the wave does possess very rapidly decaying (doubly exponential) tails.

In simulations and experiments, one can generate a traveling wave in a granular chain by impacting one boundary of the chain (which is at rest) with some initial velocity  $v_i$ . Using scaling arguments on the quasicontinuum model (15), one can show that  $c \propto v_i^{1/5}$  [146, sections 1.4 and 1.6.2] for Hertzian interactions. The analytical approximations that we reviewed in this section are consistent with experimental and numerical findings [39, 40, 116]. Such results are now considered classical, and numerous studies on traveling waves in granular chains have followed them and built upon them. See the review article [176], which is

dedicated to solitary-wave solutions of granular chains. In the remainder of this article, we will emphasize results that appeared after [176].

## 5.2. Genuine traveling solitary waves

The experiments, numerical simulations, and informal asymptotics that we discussed in section 5.1 all suggest the existence of stable traveling solitary-wave solutions in a homogeneous granular chain. In this section, we consider the fundamental mathematical issue of the existence of *genuine* traveling waves. Genuine traveling waves are solutions that travel through a granular chain without any disturbance to the original wave shape. To identify genuine traveling wave solutions, it is convenient to work directly in the strain-variable formulation of equation (6). Substituting the ansatz  $y_n(t) = \Phi(n - ct, t) = \Phi(\xi, t)$  into equation (6) yields

$$\begin{aligned} \partial_t^2 \Phi(\xi, t) = & -c^2 \partial_\xi^2 \Phi(\xi, t) + 2c \partial_\xi t \Phi(\xi, t) \\ & + \{ [\delta_0 + \Phi(\xi - 1, t)]_+^{3/2} - 2[\delta_0 + \Phi(\xi, t)]_+^{3/2} \\ & + [\delta_0 + \Phi(\xi + 1, t)]_+^{3/2} \}. \end{aligned} \quad (17)$$

Traveling waves of equation (3) correspond to stationary (i.e. time-independent) solutions  $\Phi(\xi, t) = \phi(\xi)$  of equation (17). Such solutions satisfy

$$\begin{aligned} 0 = & -c^2 \partial_\xi^2 \phi + \{ [\delta_0 + \phi(\xi - 1)]_+^{3/2} - 2[\delta_0 + \phi(\xi)]_+^{3/2} \\ & + [\delta_0 + \phi(\xi + 1)]_+^{3/2} \}. \end{aligned} \quad (18)$$

If the solution also has the property that  $\lim_{\xi \rightarrow \pm\infty} \phi(\xi) = 0$ , it is called a ‘solitary wave’. The existence of such solutions follows from a general result of Friesecke and Wattis [69], which holds for traveling wave solutions of general FPU lattice equations. In [133], this result was applied to equation (6). Although this existence result is exact (no approximations were made), this proof of it is not constructive, so analytical approximations like (16) and numerical computations are very useful. Chatterjee argued heuristically in [31] that the tails of this genuine traveling wave solution are doubly exponential rather than truly compact (as suggested by the continuum approximation of equation (16)) when there is no precompression. This fact was proved subsequently in [55] by formulating the advance–delay equation (18)

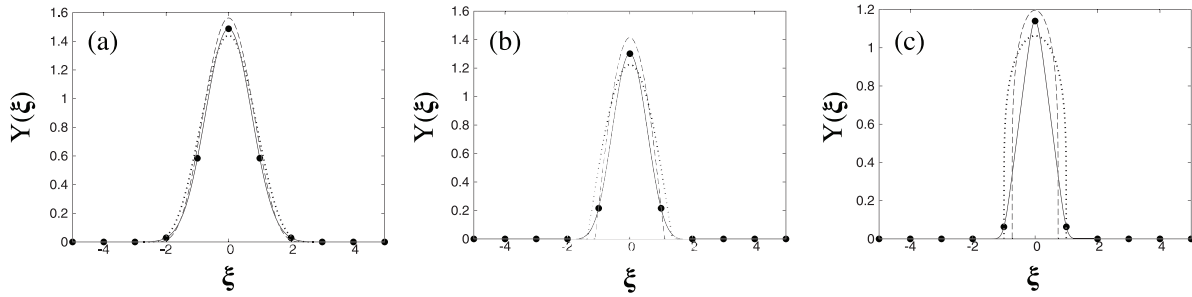


**Figure 5.** Comparison of continuum approximations and genuine solitary-wave solutions of equation (6) for (a)  $p = 3/2$ , (b)  $p = 3$ , and (c)  $p = 11$ . The markers show the wave on the lattice, dotted curves show the corresponding solutions of the continuum model (23), and dashed curves show equation (16). The approximation does poorer as the nonlinearity exponent  $p$  increases. Reprinted figure with permission from [7], Copyright (2009) by the American Physical Society.

(with  $\delta_0 = 0$ ) as a fixed-point problem: Using the transform  $\phi(\xi) = \int_{-\infty}^{\infty} \hat{\phi}(k)e^{ik\xi}dk$  leads from equation (18) to

$$\hat{\phi}(k) = \frac{1}{c^2} \text{sinc}^2\left(\frac{k}{2}\right) \widehat{\phi^{3/2}}, \quad (19)$$

where the hat  $\hat{\phantom{x}}$  denotes the (wavenumber-dependent) Fourier transform of the spatial variable. Invoking the convolution theorem yields

$$\phi(\xi) = \Lambda(\xi) * \phi^{3/2} = \int_{-\infty}^{\infty} \Lambda(\xi - y)\phi^{3/2}(y)dy, \quad (20)$$

where  $\Lambda(\xi) = (1/c^2) \max\{1 - |\xi|, 0\}$ . Without loss of generality (given the scaling properties of equation (6)), one can assume that  $c = 1$ . Using  $z = \xi - y$  and changing variables in (20) then yields

$$\begin{aligned} \phi(\xi + 1) &= \int_{-1}^1 \Lambda(z)\phi^{3/2}(\xi + 1 - z)dz \leq \phi^{3/2}(\xi) \\ &\Rightarrow \phi(\xi + n) \leq \phi(\xi) \left(\frac{3}{2}\right)^n, \end{aligned} \quad (21)$$

where we used only the fact that  $\sup_{y \in [-1, 1]} \phi^{3/2}(\xi + 1 - y) = \phi^{3/2}(\xi)$  for a positive, monotonically decreasing traveling wave (and the normalization  $\int_{-1}^1 \Lambda(z)dz = 1$ ). This establishes the doubly-exponential decay for traveling solitary waves in granular chains with a Hertzian potential  $p = 3/2$ , and it shows for general exponents  $p$  that  $\phi_n \sim \phi_0^{p^n}$  as  $n \rightarrow \infty$ . Equation (20) also provides an efficient numerical algorithm for the computation of such waves by setting up a fixed-point iteration scheme (see [55, section 4]). Using an iterative scheme in Fourier space (e.g. equation (19)) for the computation of solitary waves in the context of FPU lattices was first introduced in [84]. Stefanov and Kevrekidis [184] used a reformulation of equation (20) to prove the existence of bell-shaped, monotonically decaying traveling waves for  $\xi > 0$  by constructing an energy functional for which the constrained minimization problem over bell-shaped entries has a solution. The proof was generalized in [185] for granular chains with nonzero precompression. In the latter scenario, the precompression absorbs most of the decay in the estimate of equation (21), leaving  $\phi(\xi + 1)$  bounded above by  $\phi(\xi)$  multiplied by a suitable prefactor. Decay in this case is thus exponential, as observed both numerically and experimentally [146]. The associated waves

are strongly reminiscent of the supersonic waves of standard FPU chains [185]. Moreover, the speed of sound is related to the precompression:  $c_s \propto \sqrt{p} \delta_0^{p-1}$ , in line with the characterization of the  $\delta_0 = 0$  case as a ‘sonic vacuum’ [146]. We will further discuss granular chains with precompression in section 5.4.

One can study the stability of stationary solutions  $\phi^0$  of equation (18) by examining the fate of small perturbations around them. More concretely, one substitutes the linearization ansatz  $\Phi(\xi, t) = \phi^0 + \varepsilon a(\xi)e^{\lambda t}$  into equation (17) to obtain the eigenvalue problem

$$\begin{aligned} \lambda^2 a(\xi) &= -c^2 \partial_\xi^2 a(\xi) + 2\lambda c \partial_\xi a(\xi) + \frac{3}{2} \{[\delta_0 + \phi^0(\xi - 1)]_+^{1/2} a(\xi - 1) \\ &\quad - 2[\delta_0 + \phi^0(\xi)]_+^{1/2} a(\xi) + [\delta_0 + \phi^0(\xi + 1)]_+^{1/2} a(\xi + 1)\}. \end{aligned} \quad (22)$$

A similar formulation was used to study the stability of traveling kink solutions of the sine-Gordon equation [101]. The stability properties of genuine solitary-wave solutions are unknown from a mathematically rigorous perspective, although both direct numerical simulations and experiments suggest overwhelmingly that they must be stable [146, 204]. Moreover, it is not even clear if the stability characteristics of stationary solutions of the advance–delay equation (17) are inherited by the corresponding solutions of the discrete equation (6). More generally, this is an important question about the stability of traveling waves on lattices, as the model in equation (17) contains spatial scales that are in some sense ‘inaccessible’ to the original lattice (i.e. ones that are below the scale of the lattice spacing). Consequently, one can, in principle, envision a scenario in which equation (17) includes instabilities whose imprint cannot occur in the original system in equation (6).

In the absence of rigorous mathematical results, numerical computations give another route to gather information on the stability of traveling waves in granular chains. One then requires a numerical approximation of equation (18), which one can achieve by discretizing equation (18) in the variable  $\xi$  and employing Newton iterations to approximate the solution [53, 204, 210]. Upon this discretization, equation (22) becomes a standard matrix eigenvalue problem. One must be cautious, however, because the discretization can introduce spurious eigenvalues [210, 216]. Indeed, the best choice of discretization for stability computations is also an open problem.

An important complementary approach to understanding the stability of a traveling wave solution of equation (6) through analysis of equation (17) that respects the underlying discreteness of the lattice model is to consider traveling waves as periodic orbits imposed at the level of the original lattice [67]. In other words, they are fixed points of the dynamical evolution process of travel by one site followed by an integer shift of the sites. This viewpoint was explored for traveling breathers in [75]. In our view, pursuing both of these approaches (discrete versus continuum), comparing their spectra (see also the recent work of [53]), and appreciating their similarities and differences is a crucial open area in the mathematical analysis of traveling waves in discrete Hamiltonian systems.

### 5.3. Other continuum models and their limitations

Although the agreement between the quasicontinuum approximation (15) and numerical computations seems satisfactory for the exponent  $p = 3/2$ , the level of agreement becomes progressively less satisfactory as  $p$  increases, as was discussed systematically in [7] (see figure 5). Consequently, it is natural to ask if it is possible to derive the quasicontinuum model of equation (3) in a mathematically rigorous way—for example, by bounding the error of the approximation in a suitable norm in terms of some small parameter. Using the scaling  $Y(\epsilon n, \epsilon t) = Y(X, T)$ , one can derive the following continuum model from the strain-variable formulation (6) of a granular chain [7, 38, 84, 202]:

$$\partial_T^2 Y = \partial_X^2(Y^p) + \frac{\epsilon^2}{12} \partial_X^4(Y^p). \quad (23)$$

Like equation (16), the model (23) also possesses solutions with compact support. Equation (23) is a strongly nonlinear model reminiscent of the Boussinesq equation. Both equation (15) and equation (23) are pathological in the sense that they are ill-posed for  $p = 1$  because of large-wavenumber instabilities in the associated dispersion relation  $\omega^2 = k^2 - \frac{\epsilon^2}{12} k^4$  [47]. The fact that instabilities at large  $k$  lead to ill-posedness of equation (23) has been studied both numerically and by demonstrating instability of the compact solutions [94]. Alternative paths [168, 169] (see also [146, section 1.4]) for ‘regularizing’ these equations are possible. For example, one can write

$$\partial_T^2 Y = \partial_X^2(Y^p) + \frac{\epsilon^2}{12} \partial_X^2 \partial_T^2(Y^p) \quad (24)$$

by inverting  $1 - \frac{\epsilon^2}{12} \partial_X^2$  in equation (23) and Taylor expanding it on the left-hand side. However, equation (24) also has issues, as now traveling waves acquire an exponential tail [93] and thus do not possess the proper doubly-exponential decay [55, 184]. It is also interesting (and an open avenue) to consider a variant of equation (23) involving Padé approximations [104, 168, 169, 202] of the form

$$\partial_T^2 Y = \frac{\partial_X^2}{1 - \frac{\epsilon^2}{12} \partial_X^2} Y^p. \quad (25)$$

As an aside, we note that one can directly approximate the solitary traveling wave of equation (3) using a Padé approximation by substituting the ansatz

$$\phi(\xi) = \frac{1}{\sum_j q_j \xi^j}$$

into a normalized variant of equation (18) and solving an algebraic system for the  $q_j$  [183]. The continuum models above are somewhat unsatisfactory, as they require an arbitrary truncation in the Taylor expansion of the nonlinearity. A more mathematically sound approach is possible by defining  $p = 1 + \epsilon$  and considering an approximation in the  $\epsilon \rightarrow 0$  limit (i.e. in the vicinity of the linear limit). One thereby derives the so-called ‘log-KdV equation’ [93]

$$\partial_T Y + \partial_X^3 Y + \partial_X(Y \log(|Y|)) = 0 \quad (26)$$

using the scaling  $Y(\epsilon(n-t), \epsilon^3 t) = Y(X, T)$ . Equation (26) possesses an exact Gaussian traveling wave solution. The exact solitary-wave solution of equation (18) and the compacton solution of (23) both approach this Gaussian profile in the  $\epsilon \rightarrow 0$  limit for near-sonic wave speeds. However, the Gaussian traveling wave does not capture the doubly-exponentially decaying coherent structure as  $p$  deviates from 1 (and especially for  $p = 3/2$ , where it fails by about 35%). It is unclear if equation (26) is well-posed, as the nonlinear term diverges at  $Y = 0$ . Consequently, a full understanding of continuum modeling of a purely nonlinear granular chain remains a difficult problem that has only partially been addressed.

### 5.4. Traveling solitary waves in precompressed Granular chains

If a granular chain is compressed statically (such that  $\delta_0 \neq 0$ ), its governing equation (3) is linearizable, and the resulting dynamics differ strikingly from the case without precompression. As we indicated previously (see section 5.2), the supersonic waves in this case possess tails with an exponential decay (rather than the doubly-exponential decay of a purely nonlinear granular chain). This implies that the traveling wave solution of the purely nonlinear problem is a singular limit—rather than a regular limit—of the traveling wave solution as the precompression tends toward 0.

In the presence of precompression, the scaling  $Y(\epsilon(n-t), \epsilon^3 t) = Y(X, T)$  leads to another log-KdV equation, similar to equation (26), that is well-posed (because the nonlinear term is no longer divergent) [54]. This variant of the log-KdV equation is a useful model for general initial data, as opposed to equation (26), which is relevant only for special solutions. A rigorous justification of this log-KdV equation as an accurate continuum limit of a granular chain with precompression (defined in equation (6)) was given in [54].

Adding precompression also introduces a natural small parameter  $|y_n/\delta_{0,n}| \ll 1$  for the strain amplitude  $y_n$  relative to the precompression value  $\delta_{0,n}$ . For solutions with small strain magnitude  $|y_n|$ , the nonlinear response is weak, and one can describe the dynamics of a granular chain through its associated Taylor expansion. Continuum modeling of the FPU equation with a polynomial potential is well-understood [65, 174]. For example,

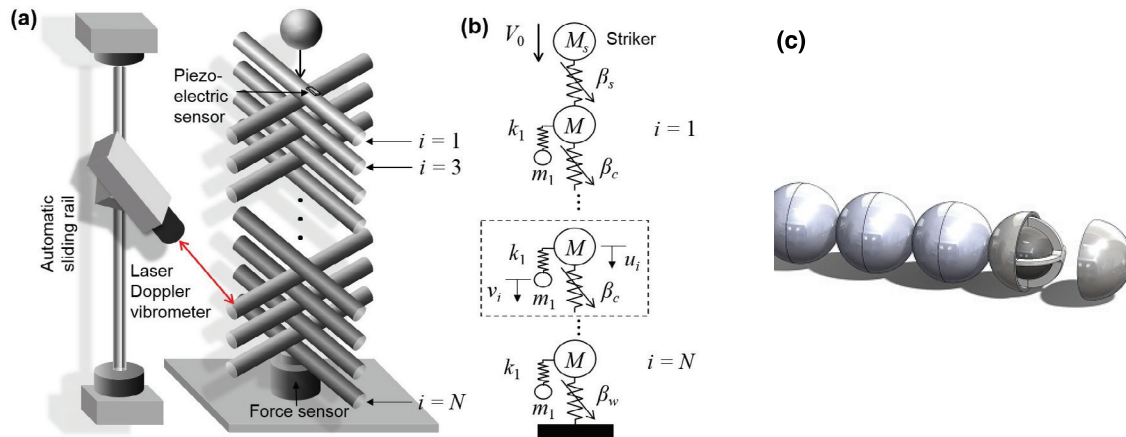


**Figure 6.** (a) A woodpile chain, which can be modeled as (b) a locally resonant granular crystal. (a) and (b) Reprinted figure with permission from [110], Copyright (2015) by the American Physical Society. (c) A mass-in-mass granular chain. Reproduced with permission from [43].

using the scaling  $y_n = \epsilon^2 Y(\epsilon(n - ct), \epsilon^3 t) = \epsilon^2 Y(X, T)$  applied to a precompressed granular chain with the first three terms in its Taylor expansion (see equation (10)) leads to the Korteweg–de-Vries (KdV) equation [212]

$$2c\partial_T Y = \frac{c^2}{12}\partial_X^3 Y + K_3\partial_X(Y^2), \quad (27)$$

where one chooses  $\delta_0$  so that  $K_2 = 1$ . The soliton solution of the KdV equation (27) provides a reasonable approximation of the genuine traveling solitary-wave solution of a precompressed granular chain for velocities  $c$  close to (but above) the sound speed  $c_s$ . Solitary-wave interactions have also been explored in this context [177]. The KdV description has been studied rigorously (with error estimates) for a monomer FPU chain [65, 174]. In stark contrast to granular chains without precompression, there are rigorous results not only for the existence of traveling solitary waves but also in descriptions of both their linear and nonlinear stability [66–68]. Additionally, [32, 70] rigorously derived the KdV equation for dimer and  $M$ -mer granular chains (see section 5.5).

### 5.5. Traveling structures in configurations other than monomer chains

Let us now discuss striking the end of a heterogeneous (i.e. nonuniform) granular chain. Generically, for heterogeneous chains, one does not observe the formation of a constant-shape traveling structure that propagates indefinitely (as in figure 4). For example, for a diatomic granular chain that consists of alternating light and heavy masses, the lighter-mass particles vibrate between adjacent particles of heavier mass after the initial wave front has passed. This can result in the attenuation of a traveling wave. Hence, although early numerical and experimental (and heuristic analytical) studies for diatomic (and triatomic) granular chains suggested the possible existence of propagating structures [161, 162], a more systematic examination of the dynamics revealed an intriguing phenomenology that depends on the ratio of light to heavy masses [95]. This ratio is a canonical parameter of a diatomic chain, and pulse attenuation can be significant at special mass ratios (i.e. at ‘resonances’) [95, 96],

as has been studied both theoretically [96] and experimentally [109, 201]. Interestingly, for another set of special mass ratios (i.e. at so-called ‘anti-resonances’) [95], there seems to exist a genuine traveling wave structure, as the vibrating frequency of the lighter particles is in synchrony with the wave speed of the traveling structure, so energy is transferred completely from the lighter to the heavier particles and vice versa. This latter feature has also been confirmed experimentally [109]. (See [197] for the related case of a diatomic Toda lattice.) In contrast to the solitary waves of a monomer chain, the tails of a solitary wave in a dimer have small-amplitude oscillations that do not decay to 0 [95, 162]. It is an open problem if there are indeed special mass ratios in which the oscillating tails vanish (i.e. if there exists a genuine solitary wave with exponentially decaying tails in diatomic granular chains). This question has been answered partially in the related problem of a diatomic FPU problem with a polynomial potential [59]. There, it was shown rigorously that solitary waves exist near sonic speed and that they are the superposition of a periodic traveling wave (the tail) and an exponentially localized function. However, [59] did not give a lower bound for the amplitude of the periodic traveling wave, so one cannot guarantee that this ‘oscillating tail’ is nonzero for all mass ratios. Their result applies to a precompressed granular chain, but the methodology in [59] cannot be used for a purely nonlinear granular chain. The exact numerical computation of solitary waves with nonvanishing tails in a granular crystal is an intriguing open problem, and it is also open to perform systematic numerical illustrations of this phenomenon, if it exists, in the strongly nonlinear limit.

A variety of similar features to the ones that we described in the paragraph above arise in ‘locally resonant chains’, in which each particle is connected to a vibrating (resonator) element (see figure 6). For a linear resonator, the equations of motion are

$$m_n \ddot{u}_n = A_n [\delta_n + u_{n-1} - u_n]_+^{3/2} - A_{n+1} [\delta_{n+1} + u_n - u_{n+1}]_+^{3/2} - k_1(v_n - u_n), \quad (28)$$

$$\ddot{v}_n = k_1(v_n - u_n), \quad (29)$$

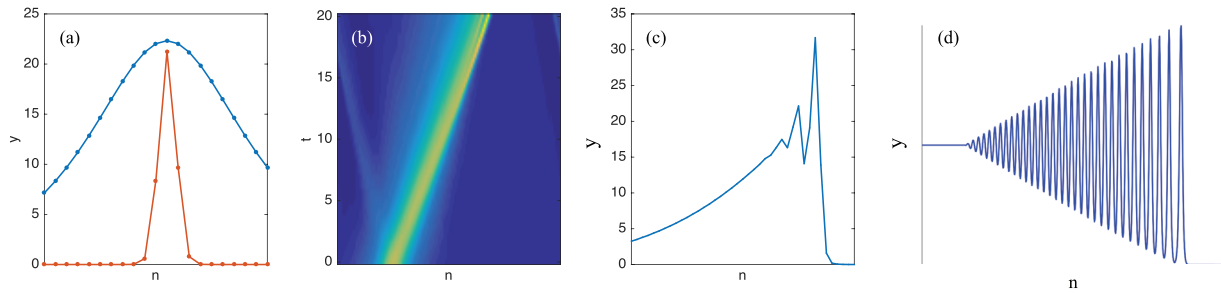


**Figure 7.** (a) Strain profile of a solitary-wave solution (red curve) in a granular chain. One uses an arbitrary long-wavelength bell-shaped curve (blue curve) as initial data when solving equation (6). (b) Contour plot of the evolution of the blue curve of panel (a) via equation (6). Observe that the high-amplitude portion of the wave (yellow) travels faster than the low-amplitude part (light blue). (c) Strain profile (at time  $t = 20$ ) showing the onset of microscopic oscillations, which are reminiscent of a dispersive shock. (d) Dispersive-shock solution of the KdV equation. Reproduced with permission from [2].

where  $v_n$  is the displacement of the attached resonator (whose mass we have scaled to 1 in equation (28)). Physical examples of locally resonant chains include ‘woodpile’ phononic structures (see figure 6), which consist of a stacked array of cylinders (i.e. rods), whose bending modes are modeled as vibrating elements [110]; ‘mass-with-mass’ systems (in which the resonators are external rather than internal) [72, 106]; and ‘mass-in-mass’ systems (in which each particle contains another vibrating particle) [21, 106]. Solitary-wave solutions of locally resonant chains are similar to their counterparts in diatomic granular chains. Generically, they have nonvanishing oscillating tails [204], but their tails do vanish for some special parameter values. See [204] for numerical computations and [105] for a rigorous proof. The woodpile chains also have another interesting characteristic: because the resonators in this case are ‘intrinsic’ (i.e. they consist of the vibrational modes of the rods themselves), one can adjust the length (and other properties) of the cylinders to tune the associated internal vibration modes. A scenario in which multiple such modes are involved in the dynamics was broached in [110], and it seems to lead typically to attenuation of wavelike excitations.

Traveling waves in heterogeneous granular chains with nonperiodic arrangements also exhibit interesting phenomena. The effect of impurities on traveling waves in granular chains is well-studied and results in reflected and transmitted waves [176]. Intriguingly, in the presence of multiple impurities (as well as precompression), the dynamics can feature resonant interactions that enable (perfect) transmission of small-amplitude waves through the impurities. This analog of the well known Ramsauer–Townsend resonance in quantum physics was illustrated recently in [137]. Another type of heterogeneous chain is a tapered one, in which some feature (e.g. the mass) of the particles increases or decreases gradually along a chain (see, e.g. [50, 51, 79, 80]). One can also design particular heterogeneities to mitigate forces at the end of a chain [64]. While the quasicontinuum modeling described in section 5.1 cannot be applied to such situations, one can obtain analytical approximations by employing the so-called ‘binary collision approximation’, in which at each time one considers the dynamics at only two lattice sites [127].

Another intriguing direction of intense recent interest involves the interplay of structural disorder with the granular nonlinearity and the lattice discreteness. In the broad

context of condensed-matter physics, disorder (e.g. in the form of randomness) causes strong localization—so-called ‘Anderson localization’—that affects the diffusivity of waves in disordered media [9, 22]. Recent studies in the context of granular crystals have demonstrated computationally that such localization phenomena can be altered dramatically and can be even reversed (as superdiffusive transport can occur) by manipulating the nonlinearity strength in mechanical systems [6, 136] (see also, e.g. [160, 180]) and its potential ‘competition’ with disorder. Such versatile dynamics associated with disorder and nonlinearity have been studied only very recently in granular crystals (and, more generally, they have not been studied much in lattice systems with inter-site interactions). There are numerous exciting directions to pursue in this area. Some of these predictions have now been verified experimentally [111], but additional experimental efforts are needed. A far more detailed understanding exists for lattice systems with on-site nonlinearities [61, 114], where nonlinearity promotes localization (in the form of discrete breathers), rather than enabling mobility (in the form of traveling waves, as in FPU-type lattices). As a result, energy transport is only subdiffusive, whereas (as indicated above) superdiffusivity can occur for disordered granular crystals [6, 136]. The study of disorder and nonlinear analogs of Anderson localization are important directions to pursue. They are accessible experimentally, and a systematic theoretical understanding of associated superdiffusive and subdiffusive transport should yield important insight more generally on the interaction between disorder and nonlinearity.

## 6. Dispersive shock waves

As we discussed in sections 5.1 and 5.3, one can derive a quasicontinuum approximation of a solitary-wave solution in a long-wavelength limit of a monoatomic granular chain. However, a genuine solitary-wave solution is strongly localized, with doubly-exponential tail decay when there is no precompression and exponential tail decay when there is precompression. If one considers a similar waveform, except with a considerably wider spatial scale (see figure 7), it appears, upon evolving the initial data through

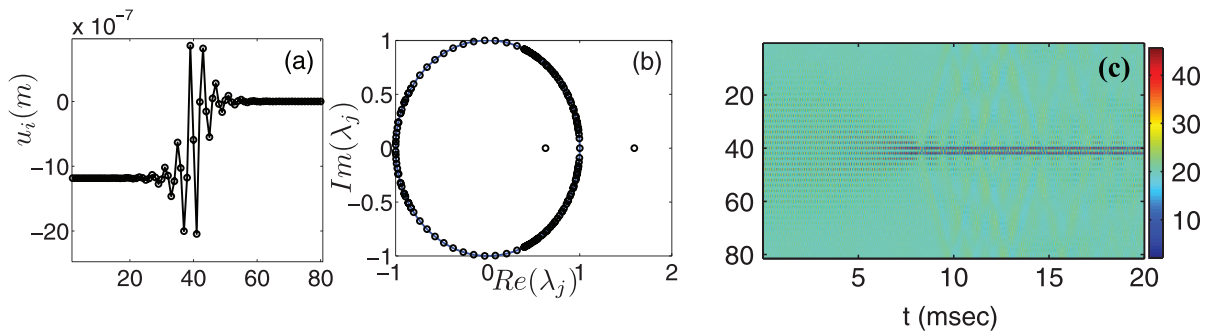


**Figure 8.** A Hamiltonian breather of a diatomic granular chain considered in [191]. (a) Profile of the displacement  $u_n$  and (b) Floquet spectrum of the solution in panel (a). There is a Floquet multiplier (FM) with modulus greater than 1, indicating that there is an instability. (a) and (b) Reprinted figure with permission from [190], Copyright (2010) by the American Physical Society. (c) Spatiotemporal evolution of the forces for a simulation of the modulation instability and ensuing breather generation from initial conditions that correspond to the lower optical cutoff (plane-wave) mode (see figure 3). Reprinted figure with permission from [20], Copyright (2010) by the American Physical Society.

equation (6), that the wave speed of each point of the wave-form depends on the amplitude at that point, with larger amplitudes entailing faster wave speeds (see figure 7(b)). To understand this observation from an analytical perspective, one can employ a quasicontinuum modeling approach [146, section 1.4.5]. We consider the long-wavelength ansatz  $y_n = Y(\epsilon n, \epsilon t) = Y(X, T)$ . This yields

$$\partial_T^2 Y = \partial_X^2 [(\delta_0 + Y)^p]. \quad (30)$$

Equation (30) is reminiscent of equation (23), except that now  $\delta_0 \neq 0$  and there is no higher-order correction term. We can rewrite equation (30) as a system of conservation laws [34]:

$$\left. \begin{aligned} \partial_T Y - \partial_X V &= 0 \\ \partial_T V - \partial_X [(\delta_0 + Y)^p] &= 0 \end{aligned} \right\}, \quad (31)$$

which have the form of a so-called ‘p-system’ [123, 179]. By defining

$$\mathbf{Y} = \begin{pmatrix} Y \\ V \end{pmatrix} \quad \text{and} \quad F(\mathbf{Y}) = \begin{pmatrix} -V \\ -(\delta_0 + Y)^p \end{pmatrix},$$

we can express equation (31) as a Burgers-type system:

$$\partial_T \mathbf{Y} + DF(\mathbf{Y}) \partial_X \mathbf{Y} = 0, \quad (32)$$

where

$$DF(\mathbf{Y}) = \begin{pmatrix} 0 & -1 \\ -p(\delta_0 + Y)^{p-1} & 0 \end{pmatrix}$$

is the Jacobian matrix of  $F$ . The eigenvalues of  $DF(\mathbf{Y})$  are  $\lambda_{\pm}(\mathbf{Y}) = \pm \sqrt{p(\delta_0 + Y)^{p-1}}$ , which suggests that solutions of equation (31) consist of traveling waves with velocity  $\pm \sqrt{p(\delta_0 + Y)^{p-1}}$ . Because the velocity depends on the amplitude  $Y$  of the solution (with larger speeds for larger amplitudes if  $p > 1$ ), bell-shaped initial data deforms and steepens, as observed in figure 7. For  $\delta_0 \neq 0$ , it was demonstrated rigorously in [34] that equation (30) accurately describes the dynamics of a granular chain over long but finite time intervals. The approximation breaks down when solutions of equation (30) become singular (e.g. at the point of wave breaking).

In the inviscid Burgers equation  $\partial_t u = \partial_x(u^2)$ , the steepening of bell-shaped initial data leads ultimately to the formation of ‘shock waves’ (i.e. front solutions that develop an infinite derivative in finite time) [52]. Such derivative singularities cannot arise in a granular chain (because it is discrete in space), but the result of the amplitude-dependent wave speed (see figures 7(b) and (c)) and subsequent steepening is reminiscent of systems that possess so-called ‘dispersive shocks’ [2], in which microscopic oscillations spread out in space and time (see figure 7(d)). Something very similar occurs in granular chains with precompression [34] (see figure 7(c)), presumably because of the dispersive role of discreteness when a structure becomes sufficiently localized in space. Recently, dispersive shocks were studied numerically in FPU lattices with general convex potentials for arbitrary Riemannian (i.e. jump) initial data [82]. Because the p-system cannot describe the microscopic oscillations observed in figure 7(c), it is necessary to pursue other avenues to study them analytically. For example, in the presence of precompression, one can consider the KdV limit (see equation (27)) and derive Whitham equations to describe the amplitude of the oscillations of a KdV dispersive shock [2]. A complementary perspective arises from identifying a first-order equation (with  $Y_T \propto (Y^{\frac{p+1}{2}})_X$ ) in a vein similar to [138] and exploring its nonlinear transport properties. One can also construct discretizations of this first-order equation and examine the properties of those discrete equations, analogous to the discretization analyses of Burgers equation in [196]. As our discussion suggests, the analytical study of dispersive shocks in granular chains both with precompression and (especially) without precompression includes a considerable number of fascinating open questions.

Shock-like structures have been studied experimentally in granular chains with  $p = 3/2$  and  $\delta_0 = 0$  [140]. In that work, a ‘shock wave’ was generated by imparting velocity continuously to the end of a chain [140]. Another work relevant for the experimental realization of shocks in granular media is [81], which considered the role of dissipation. The oscillations observed in the shock wave of the Hamiltonian system (3) disappear beyond a critical value of the viscosity of the damped system [81].

## 7. Breathers

### 7.1. Discrete breathers and their stability

The final example of a prototypical nonlinear structure in a granular chain that we will discuss is a ‘discrete breather’ (sometimes also called an ‘intrinsic localized mode’), which is temporally periodic<sup>12</sup> and strongly localized in space [28]. In the context of a granular chain, a discrete-breather (DB) solution of equation (3) satisfies the properties

$$u_n(t) = u_n(t + T_b), \quad \lim_{n \rightarrow \pm\infty} |u_n - u_{n+1}| = 0,$$

where  $T_b$  is the breather period (see figure 8(a)). Breathers are generic excitations in spatially extended, discrete, periodic (or quasiperiodic) systems [62]. The span of systems in which such structures have been studied is broad and diverse: they include optical waveguide arrays and photorefractive crystals [117], micromechanical cantilever arrays [172], Josephson-junction ladders [17, 195], layered antiferromagnetic crystals [56, 175], halide-bridged transition metal complexes [186], dynamical models of the DNA double strand [158], Bose–Einstein condensates in optical lattices [141], and many others.

Once one finds a breather solution numerically (e.g. via a fixed-point iteration of the time- $T_b$  map of a system of interest (see section 7.7), a natural followup question is its stability. There have been extensive studies of the stability properties of breathers in discrete Hamiltonian systems (see [62, 4.2] and [12, 63]). For breathers in a granular chain, we focus on the notion of ‘spectral stability’, which is determined in the following way. One adds a perturbation to a breather solution and uses equation (3) to derive an equation that describes the temporal evolution of the perturbation. Keeping only linear terms in this equation yields a Hill equation with temporally-periodic coefficients of period  $T_b$  (see equation (40) of section 7.7). Consequently, the eigenvalues (or Floquet multipliers) of the associated variational matrix  $V(t)$  at time  $t = T_b$  determine the spectral stability of breather solutions. Because of the Hamiltonian structure of the system, all Floquet multipliers (FMs) must lie on the unit circle for the solution to be (marginally) stable; otherwise, the solution is unstable (see figure 8(b)). There are continuous arcs of spectrum on the unit circle (in the infinite-lattice limit), and one can compute these arcs from the linear spectral bands of equation (3). In general, the isolated multipliers (i.e. the ‘point spectrum’) must be computed numerically (see section 7.7). For Hamiltonian systems, there is at least one pair of FMs at the point +1 (i.e. at the point (1,0) of the unit circle). These correspond to the invariance of the system under time translation—a feature responsible for the conservation of the total energy. By exploiting information about this FM pair, one can extract a stability criterion for breathers [102] that is reminiscent of the well-known Vakhitov–Kolokolov criterion for the stability of solitary waves. Specifically, this criterion establishes that a change of the monotonicity of the energy–frequency curve

results in a change of stability of the corresponding breather solution. The above notion of stability is tantamount (for states such as traveling waves) to that of linear stability around stationary or traveling structures. The persistence of breathers under fully nonlinear evolution in granular chains (and in general nonlinear lattices) is still incomplete. Therefore, at present, the above spectral-stability predictions need to be validated through direct numerical simulations.

In the presence of damping (see section 7.5), the picture is different, because then a granular chain is no longer Hamiltonian. The continuous part of the spectrum now typically lies within the unit circle, so most eigendirections of perturbation decay over time. If all FMs lie within the unit circle, the solution is not merely stable, but it also attracts nearby dynamics. Naturally, in this case, for a DB to exist in the first place, there needs to be some form of forcing (or energy pumping). Some of the examples that we will give in section 7.5 are in damped, driven granular chains. An interesting avenue for future work is to seek solutions in the form of dissipative DBs, which have been studied in systems such as radio-frequency superconducting quantum interference device arrays [115].

### 7.2. Nonexistence results

In the absence of precompression (i.e. when  $\delta_{0,n} = 0$ ), the mean interaction force of a temporally-periodic solution  $u$  must vanish:  $\int_0^T V'(u_{n-1}(t) - u_n(t))dt = 0$ . This observation, and the fact that  $-V(u_{n-1} - u_n) \leq 0$ , implies that the only temporally-periodic solutions are the trivial equilibria (see [93, theorem 1]). Consequently, for a homogeneous chain, precompression is crucial for the emergence of DBs. The linear band structure that results from precompression allows a natural place from which breathers can bifurcate. In a monomer granular chain, one can try to construct approximate breather waveforms using a continuum modeling approach. With the ansatz

$$\begin{aligned} y_n(t) &\approx \epsilon Y(X, T) \exp(ik_0 n + i\omega_0 t) + \text{c.c.} + \text{h.o.t.}, \\ X &= \epsilon(n - ct), \quad T = \epsilon^2 t, \end{aligned} \quad (33)$$

where ‘c.c.’ is the complex conjugate and ‘h.o.t.’ stands for higher-order terms, one can derive a nonlinear Schrödinger equation (NLS) from equation (6)<sup>13</sup>. The NLS that one obtains is

$$i\partial_T Y = \nu_2 \partial_X^2 Y + B|Y|^2 Y, \quad \nu_2 = -\omega''(k_0)/2 > 0, \quad (34)$$

where  $B$  is a lengthy wavenumber-dependent expression [89, 173]. We define the notation  $\omega_0 = \omega(k_0)$ , where  $k_0$  is the wavenumber and  $\omega(k_0)$  is the angular frequency given by the dispersion relation (13) evaluated at the wavenumber  $k_0$ . We also introduce the notation  $c = \omega'(k_0)$ . The approximation (33)

<sup>13</sup>Note that the NLS ansatz (33) assumes small amplitudes, so one actually derives the NLS equation from the FPU model with a polynomial potential given by a Taylor expansion of the Hertz law (10). This is similar to the derivation of the KdV equation in section 5.4.

<sup>12</sup>Arguably, it may be desirable to loosen the definition and not demand strict periodicity.

represents a standing DB if  $c = 0$  (i.e. when the dispersion curve has vanishing slope). For a granular chain, this occurs at the edge of the spectrum (i.e. at  $k_0 = \pi$ ). At the wavenumber  $k_0 = \pi$ , the coefficient  $B$  is

$$B = 3K_2K_4 - 4K_3^2. \quad (35)$$

For any value of the nonlinearity exponent  $p > 1$ , one obtains  $B < 0$  for a granular chain. The ansatz (33) represents a spatially-localized function if the envelope function  $Y$  is spatially localized. The soliton solution of the NLS equation (34) is a spatially localized function, but this solution exists only for the focusing NLS equation (i.e. when  $B > 0$ ). This suggests the possibility that breathers (of small amplitude and on top of a vanishing background) may not exist in a monomer granular chain. (As with other coherent structures and motivated by optical systems, breathers on top of a vanishing background are sometimes called ‘bright’ breathers.) One can reach the same conclusion by realizing that linear plane-wave solutions that evolve through the nonlinear equations of motion can collapse to a localized breather state through a modulational instability (MI) of a homogeneous background. For the monomer  $K_2$ – $K_3$ – $K_4$  FPU lattice, the condition for MI of plane waves is  $3K_2K_4 - 4K_3^2 > 0$  [62, section 4.3]. The expression on the left-hand side of this inequality is exactly the nonlinearity coefficient of the NLS equation (35). Because  $B < 0$ , breathers cannot form through an MI. This discussion thus gives a heuristic argument that bright breathers do not exist. This result has been made mathematically rigorous using center-manifold theory [90], a rather different approach from the investigation of MIs. This result implies that to obtain a breather in a granular chain, one must modify the configuration either by altering the chain (e.g. with a heterogeneity or an on-site potential) or by seeking an alternative waveform (e.g. seeking a dark breather rather than a bright breather, as described in section 7.6). In the following sections, we will explore both scenarios.

### 7.3. *Breathers in chains with impurities*

By introducing an impurity (or ‘defect’) into a precompressed (and hence linearizable) monomer granular chain, one can create a linear mode from which a breather can bifurcate. Such breathers are sometimes called ‘impurity modes’. It is possible to construct one or more breather branches as nonlinear continuations of (light-mass) defect modes of the linear problem. One can compute the eigenfrequencies and their modes as described in section 4. If the defect mass is lighter than the other masses in the ‘host’ chain, the corresponding eigenfrequency lies above the acoustic band, so the corresponding mode is spatially localized [134]. Otherwise, the eigenfrequency lies within the acoustic band, and the associated mode is spatially extended. In [191], it was shown using a granular chain with free boundary conditions and a single light defect that breathers can be continued in frequency from the localized linear defect mode to the edge of the acoustic band. The solutions feature a profile that is asymmetric. The case of two identical defects is qualitatively similar to the single-defect case if the defects are adjacent. However, if there is a particle

between the two defects in a chain, there exists both a linear defect mode with a symmetric profile and a linear defect mode with an antisymmetric profile. The branch corresponding to the continuation of the antisymmetric mode undergoes a symmetry-breaking pitchfork bifurcation in which two asymmetric solutions are created. If the two defects are different (e.g. in their masses), the antisymmetric branch undergoes an imperfect pitchfork bifurcation.

### 7.4. *Breathers in periodically-arranged chains*

One obtains a periodic arrangement in an infinite granular chain by introducing an infinite number of defects in a periodic fashion. (The simplest example is a diatomic chain.) However, in contrast to a chain with a finite number of impurities, the linear mode from which a breather bifurcates is not spatially localized. Instead, a DB forms spontaneously after a spatially extended linear plane wave undergoes an MI (see figure 8(c)). In the context of granular chains, DBs were first studied theoretically and illustrated experimentally in [20] using precompressed diatomic chains that consisted of alternating steel and aluminum spheres. A chain was driven at the boundaries at the first cutoff frequency of the optical band, and the corresponding mode experienced an MI. This occurred because the bottom of the optical band of the dispersion relation satisfies  $\omega''(k_0) > 0$  (see figure 3(a)), which leads through an asymptotic reduction to an effectively self-focusing NLS equation<sup>14</sup>, which is subject to an MI. After some transient dynamics, a breather (spontaneously) forms, and it has a frequency that is located in the spectral gap that joins the acoustic and optical bands. One can obtain a more precise description of such a breather through numerical computations and subsequent parametric continuation. Several families of DB solutions in diatomic granular chains were studied in [190]. These breathers have different amplitudes and amounts of localization, and they can be either asymmetric or symmetric. The asymmetric breathers are centered at a light particle, and the symmetric ones are centered at a heavy particle. If the DB frequency is sufficiently close to the optical band, one can approximate the breather dynamics using the NLS equation [32, 88] (in a similar vein as we described in section 7.1). The selection of both the frequency and the location of the resulting breather when it emerges as a result of instability is still an open problem.

There have also been studies of breathers in chains with larger spatial periods. For example, period-3 (i.e. ‘trimer’) chains and period-4 chains were examined in [86]. Such sequences can consist either of particles that are all distinct (such as a trimer with one steel, one aluminum, and one brass particle) or can include multiple instances of a given type of particle (such as a tetramer of one steel and three aluminum particles). The trimer and tetramer chains have, respectively, two and three spectral gaps. A surprising, generic feature of the breathers in these systems is that the ones that bifurcate from the upper bands tend to be more robust (in terms of stability) than their counterparts that bifurcate from the lower bands. This appears to be because the former are able to avoid

<sup>14</sup> Recall that, at the edge of the spectrum  $k_0 = \pi$ , the sole branch of the dispersion relation in a monomer chain satisfies  $\omega''(k_0) < 0$ .

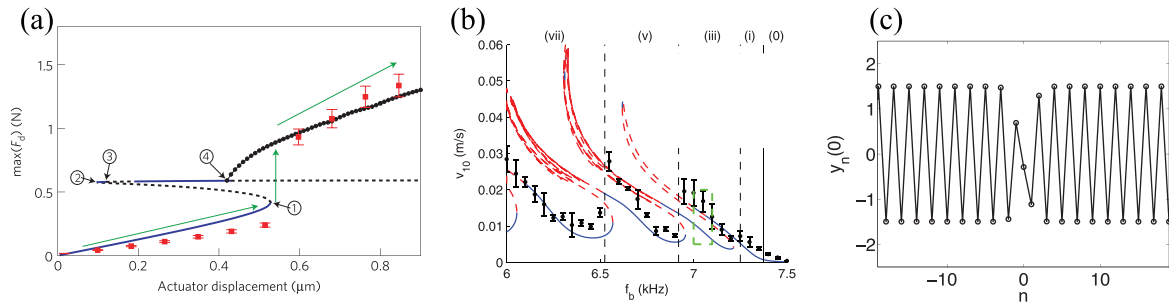


**Figure 9.** (a) Continuation in driving amplitude of a damped, driven granular chain with an impurity near the drive source. Adapted by permission from Macmillan Publishers Ltd: [Nature Materials] [19], Copyright (2010). (b) Continuation in driving frequency in a damped, driven monomer chain. Reprinted figure with permission from [37], Copyright (2014) by the American Physical Society. (c) Dark breather in a monomer granular crystal. Reprinted figure with permission from [35], Copyright (2013) by the American Physical Society.

resonances with (higher-frequency) linear modes, but a systematic investigation of the stability of the various breathers remains an open problem.

### 7.5. Breather variants in damped, driven granular chains

To obtain a more realistic description of breathing solutions from experiments of granular chains, one needs to account for their external drive and damping. Perhaps the simplest damped, driven model involves replacing one or both boundaries with a harmonic drive  $u_0(t) = a \sin(2\pi ft)$ , where  $a, f \in \mathbb{R}$ , and to add a (linear) dashpot term  $-(m_n/\tau)\dot{u}_n$  to equation (3), where the ‘inverse damping strength’  $\tau$  (which is usually determined empirically) represents a time scale associated with the damping. One can interpret this form of dissipation as friction between individual grains and the supporting rods. This model for dissipation has been used for granular chains in several previous works [19, 30, 37], although (as noted in section 3) several studies (see, e.g. [29, 76, 81, 199]) have considered internal friction caused by contact interaction between grains.

Unlike in the associated Hamiltonian model, temporally-periodic solutions of a damped, driven granular chain can attract other types of dynamics, so one can obtain them by driving an initially at-rest chain for a sufficiently long time. These are the most straightforward breather-like solutions to detect experimentally. For theoretical considerations and to obtain a more complete view of the solution space of the system, one can also obtain unstable waveforms via Newton iterations (see section 7.7). One can study the resulting solutions as one varies the driving amplitude parameter  $a$  or some other parameter. Through numerical simulations and experiments, it has been shown in a chain with an impurity [19] and periodic arrangements (e.g. driven diatomic and triatomic chains [30, 87]) that the interplay of nonlinear surface modes with modes caused by the driver create the possibility, as the driving amplitude is increased, of hysteretic dynamics and saddle–node bifurcations of limit cycles, beyond which the dynamics of the system becomes quasiperiodic or chaotic (see figure 9(a)). In light of these features, damped, driven granular chains have been proposed for acoustic switching and rectification applications [19]. An intriguing phenomenon that is worth further investigation is that periodic orbits can arise even when the drive is applied to a chain without

precompression (i.e. in the sonic–vacuum regime). See [164] for a numerical study of this observation and [215] for an experimental study. Although the nonexistence result that we discussed in section 7.2 excludes the possibility of breathers in a purely nonlinear Hamiltonian granular chain, the works [164, 215] suggest that the presence of damping and driving allow the possibility of breathers in such chains. A rigorous proof of such a result is an open problem.

For a fixed, small driving amplitude (in particular, for  $|a| \ll \delta_0$ ), one can perform a continuation in driving frequency to obtain a single branch that has peaks corresponding to the linear resonances. In general, as the driving amplitude increases, the peaks in the bifurcation diagram bend [30, 37, 132] (see figure 9(b)) in a way that is reminiscent of the fold-over event of driven oscillators [144]. See [206] for a recent study that extends this idea to granular chains. Such nonlinear bending can be useful for applications such as energy harvesting [36].

### 7.6. Breather variants in homogeneous chain configurations

As we highlighted in section 7.2, the NLS equation (34) in a homogeneous granular chain does not have bright-soliton solutions on top of a vanishing background, because the nonlinear coefficient is negative (i.e.  $B < 0$ ). In this case, the NLS equation is self-defocusing [103], and it thus possesses dark-soliton solutions

$$Y(X, T) = \sqrt{\kappa/B} \tanh\left(\sqrt{\frac{-\kappa}{2\nu_2}} X\right) e^{i\kappa T}, \quad \kappa < 0, \quad (36)$$

which have smaller amplitude than the background. Consequently, the approximation of equation (33) with the envelope function  $Y$  chosen to be a dark soliton represents a breathing solution (with  $k_0 = \pi$ ) on top of a nonzero background (i.e. it is a ‘dark breather’):

$$y_n(t) = 2\varepsilon(-1)^n \sqrt{\frac{\kappa}{B}} \tanh\left(\sqrt{\frac{-\kappa}{2\nu_2}} \varepsilon(n - x_0)\right) \cos(\omega_b t), \quad (37)$$

where  $\omega_b = \omega_0 + \kappa\varepsilon^2$  is the frequency of the breather (see figure 9(c)). This approximation, along with numerical computations, was used to study such states in a monomer granular

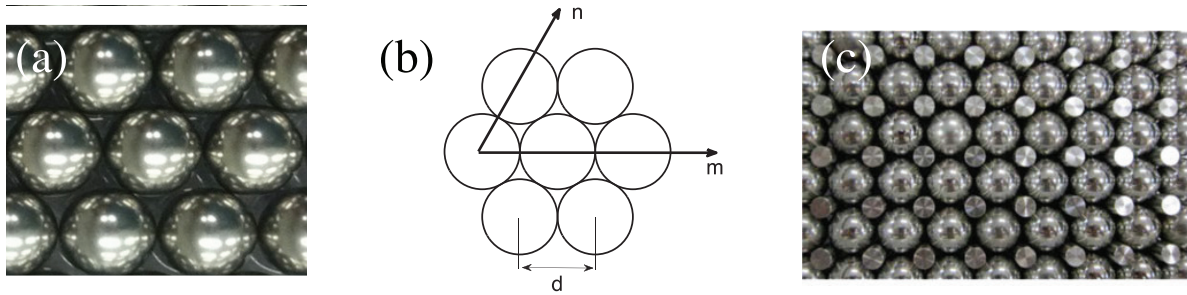


**Figure 10.** (a) A granular crystal with hexagonal packing. (b) Convention for the index orientation. The  $m$ -axis represents the horizontal direction, the  $n$ -axis represents the vertical direction, and the  $m$ -axis and  $n$ -axis meet at an angle of  $\theta = \pi/3$ . (c) A square granular lattice with cylindrical intruders. (a) and (c) Used with permission from Andrea Leonard. (b) Reprinted figure with permission from [33], Copyright (2016) by the American Physical Society.

chain in [35] for frequencies that lie within the acoustic band. For frequencies close to the cutoff frequency  $\omega_0$ , the solutions are well-approximated by the associated NLS description, and large-amplitude solutions bifurcate from the small-amplitude solutions described by the NLS equation. The experimental realization (and bistability in a damped, driven chain) of dark breathers was studied in [37]. An interesting byproduct of the investigations of bistability was the numerical and experimental identification of branches of solutions with 3, 5, 7, etc dark breathers.

Localized breathing states can also arise in a granular chain without precompression if there is an additional on-site potential. Such a model can describe systems such as an array of cantilever beams decorated by spheres or, in principle, a Newton’s cradle under the influence of gravity [92]. The breathers bifurcate from the lone linear mode introduced by the linear potential, and they tend to be more localized than the breathers that occur in granular chains with defects or periodic structures that we described in previous sections. In this setting, the breathers (and traveling generalizations of them) are well-described by the so-called ‘discrete p-Schrödinger equation’ (DpS) [91, 92, 93], which one can derive through a multiple-scale analysis similar to ones that we have described throughout this review. This multiple-scale analysis has been justified rigorously (through suitable error bounds) in this setting [91].

Breathing states have also been explored in locally resonant homogeneous granular chains (see equation (28) and figure 6) [129, 130]. In the presence of precompression, [130] examined (i) traveling bright breathers and (ii) stationary and traveling dark breathers. As with a monomer granular chain, one can use a multiple-scale expansion to derive an NLS equation—which is either of the defocusing or of the focusing variety, depending on the particular location in the acoustic or optical band—and thereby construct breathers. Perhaps more surprisingly, in granular chains without precompression, periodic traveling waves and dark breathers can exist [129], despite the absence of a linear spectrum from which these solutions can bifurcate. In this case, the relevant approximate model is a variant of the DpS equation—specifically, it is a model relying on averaging over the breather period, but which now has a considerably more complicated form than the original DpS model—rather than an NLS equation.

### 7.7. Numerical computation of breathers and their spectral stability

We now provide a brief summary of how to compute breathers in granular crystals (as well as more generally) and how to assess their stability using FMs. The primary tool used for the numerical construction of breathers is Newton fixed-point iterations [62, section 3]. We begin by writing equation (3) as a system of first order ODEs:

$$\dot{\mathbf{x}} = \mathbf{F}(t, \mathbf{u}, \mathbf{v}), \quad (38)$$

with  $\mathbf{x} = (\mathbf{u}, \mathbf{v})^T$ , where  $\mathbf{u} = (u_1, \dots, u_N)^T$  and  $\mathbf{v} = \dot{\mathbf{u}}$ , respectively, represent the  $N$ -dimensional position and velocity vectors. One then constructs a Poincaré map:  $\mathcal{P}(\mathbf{x}^{(0)}) = \mathbf{x}^{(0)} - \mathbf{x}(T_b)$ , where  $\mathbf{x}^{(0)}$  is the initial condition and  $\mathbf{x}(T_b)$  is the result of integrating equation (38) forward in time until  $t = T_b$  using standard ODE integrators [77]. A periodic solution with period  $T_b$  (i.e. satisfying the property  $\mathbf{x}(0) = \mathbf{x}(T_b)$ ) is then a root of the map  $\mathcal{P}$ . To obtain this root, one applies Newton’s method to the map  $\mathcal{P}$  in the following numerical-iteration step:

$$\mathbf{x}^{(0,k+1)} = \mathbf{x}^{(0,k)} - [\mathcal{J}]_{\mathbf{x}^{(0,k)}}^{-1} \mathcal{P}(\mathbf{x}^{(0,k)}), \quad (39)$$

where  $k$  is the index of the Newton iteration and  $\mathbf{x}^0$  is the desired root of  $\mathcal{P}$ . The Jacobian of the map  $\mathcal{P}$  is  $\mathcal{J} = \mathbf{I} - V(T_b)$ , where  $\mathbf{I}$  is the  $2N \times 2N$  identity matrix;  $V$  is the solution to the variational problem

$$\dot{V} = (DF)V, \quad (40)$$

with initial data  $V(0) = \mathbf{I}$ ; and  $DF$  is the Jacobian of the equations of motion (38) evaluated at the point  $\mathbf{x}^{(0,k)}$ . One initiates the iteration step (39) with a suitable guess (given, e.g. by a linear mode or a solution to a continuum nonlinear approximation) and applies it until one satisfies a user-prescribed tolerance criterion. One thereby obtains a temporally-periodic solution upon successful convergence (and with high accuracy). Because one must compute the monodromy matrix  $V(T_b)$  to apply Newton iterations, one immediately obtains spectral-stability information by computing eigenvalues or FMs of  $V(T_b)$ .

For a Hamiltonian granular chain (i.e. equation (3) with no damping or driving), the monodromy matrix  $V(T_b)$  has eigenvalues at  $+1$  (see the discussion in section 7.1), so the Jacobian  $\mathcal{J} = \mathbf{I} - V(T_b)$  is not invertible. To overcome this

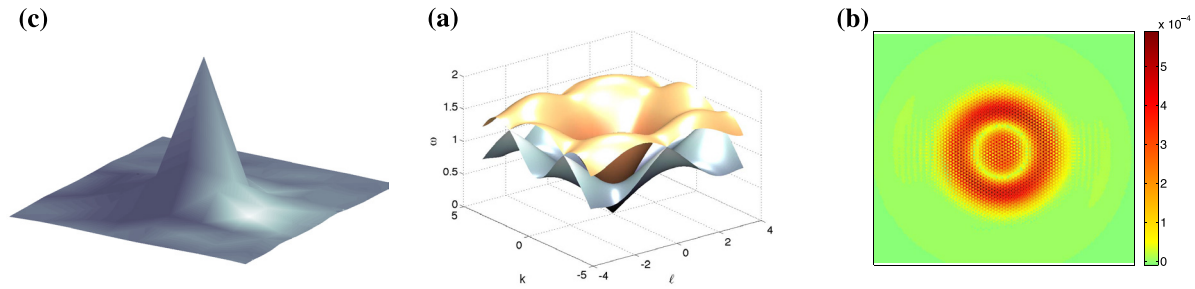


**Figure 11.** (a) A breather solution of a 2D hexagonal granular network with a single defect. We show the magnitude of the displacement. (b) Dispersion surface corresponding to equation (41). The vector of wavenumbers is  $(k, \ell)$ , and  $\omega$  is the angular frequency. (c) Conical diffraction in the 2D hexagonal granular-crystal equation (41). Such diffraction results from the excitation of linear modes near a Dirac point. (b) and (c) Reprinted figure with permission from [33], Copyright (2016) by the American Physical Society.

issue, one must break the degenerate nature of  $\mathcal{J}$  by introducing additional constraints, such as a vanishing time average (i.e.  $\int_0^T y_1(t)dt = 0$ ) or a pinning condition (e.g.  $y_1(t) = 0$ ). In practice, it can also be effective to take a pseudoinverse of  $\mathcal{J}$ . See [12] and [62] for numerous practical methods for computing the relevant periodic orbits.

## 8. Two-dimensional granular crystals

### 8.1. Packing geometries and transient dynamics

We now discuss 2D granular crystals, which have been investigated much less than the 1D configurations that we have discussed thus far. In two spatial dimensions, one can situate the nodes (i.e. particles) in a network in a large variety of ways, such as hexagonal (see figures 10(a) and (b)) or square lattices. In a square lattice, one can generate a quasi-1D traveling solitary wave by exciting the lattice along one of the spatial dimensions. This is a trivial extension of section 5, as the waves never ‘spill’ into adjacent directions. The situation for excitations in other directions is far less straightforward. However, from an experimental point of view, the square lattice is not robust structurally, because the particles can buckle readily, given the lack of contact with adjacent particles on the diagonals. One can overcome this issue by introducing ‘intruder’ particles into the vacant spaces between particles in a host crystal [187, 188] (see figure 10(c)). This is an experimentally relevant mechanism for achieving either pulse redirection [188] or (for intruders not restricted to a local area in the crystal) nonlinear pulse equipartition, a subject of intense theoretical investigation in granular crystals [187]. In the experiment of [182], two rows of granular particles were interconnected via a chain of such interstitial particles. By exciting one of the rows (the ‘impacted’ one), one can obtain an equal redistribution via the intruders between that row and the adjacent (or ‘absorbing’) row.

Without additional sources to add energy to a granular crystal, one would not expect a genuine traveling solitary wave to exist in either a square or hexagonal lattice because the energy imparted to a particle upon impact is distributed to an expanding array of neighbors as the pulse is transmitted. This process continues, leading gradually to attenuation of the wave. Consequently, many papers on granular lattices of two or more dimensions are concerned with transient

effects after a granular lattice (or more general packing) is struck [1, 13, 15, 41, 73, 118–121, 143, 150, 151, 165]; this is relevant for impact mitigation applications. Quasicontinuum approaches were explored in 2D lattices with rotation in [57]. Additionally, structured granular composites, which are networks of 1D chains arranged in 3D space, exhibit exponential stress decay [122] and can act as effective energy-dispersion mechanisms [58]. From the perspective of applications, of particular interest is a ‘sound bullet’, in which a propagating wave front is directed to specific locations in a granular crystal [181]. One can also envision scenarios in which band gaps arise in 2D granular crystals either because of heterogeneities (e.g. impurities or periodic structures) or local resonators (e.g. mass-in-mass systems). In such scenarios, it would be very interesting to explore the existence, structure, and stability properties (and more generally, the temporal evolution) of localized states in the form of DBs or their variants (e.g. impurity modes, as we discussed for 1D configurations in section 7.1). In figure 11(a), we show an example of a 2D localized mode of a 2D hexagonally packed granular lattice with a single light-mass defect in the center of the crystal. Another open problem is the study of phenomena such as ‘quasipatterns’ and ‘superpatterns’, which have often been examined for settings such as Faraday waves in fluid systems and generic amplitude equations (e.g. complex Ginzburg–Landau equations with appropriate potentials) [171, 192].

### 8.2. Hexagonal granular crystals: equations of motion, linearized dynamics, and conical diffraction

We now consider the specific case of a hexagonal granular crystal. The equations of motion account for the force at each contact point. They arise from equation (1), and each displacement  $\mathbf{q}_{m,n}$  has both a horizontal component  $u_{m,n}$  and a vertical component  $v_{m,n}$ . If the granular crystal is precompressed, the equations are linearizable. In a hexagonal monomer lattice, the equations of motion are

$$\begin{aligned} \ddot{\mathbf{q}}_{m,n} = & \mathbf{F}_1(\mathbf{q}_{m,n} - \mathbf{q}_{m-1,n}) + \mathbf{F}_2(\mathbf{q}_{m,n} - \mathbf{q}_{m,n-1}) \\ & - \mathbf{F}_3(\mathbf{q}_{m+1,n-1} - \mathbf{q}_{m,n}) \\ & - \mathbf{F}_1(\mathbf{q}_{m+1,n} - \mathbf{q}_{m,n}) - \mathbf{F}_2(\mathbf{q}_{m,n+1} - \mathbf{q}_{m,n}) \\ & + \mathbf{F}_3(\mathbf{q}_{m,n} - \mathbf{q}_{m-1,n+1}), \end{aligned} \quad (41)$$

which takes into account the six contact points from the hexagonal symmetry. We set the mass to 1 for notational simplicity. The vector-valued functions  $\mathbf{F}_j(\mathbf{q}) = \mathbf{F}_j(u, v) = [F_{j,u}(u, v), F_{j,v}(u, v)]^T$  (with  $j \in \{1, 2, 3\}$ ) have the form given in equation (1) and take into account the relative positions of the particles in contact. For example, the force along the horizontal axis that results from contact between particles at positions  $\{m, n\}$  and  $\{m, n - 1\}$  is  $F_{2,u}(u, v) = A[d - s]_+^{3/2} (d - \delta_0)(\cos(\theta) + u)/s$ , where  $s = \sqrt{((d - \delta_0)\cos(\theta) + u)^2 + ((d - \delta_0)\sin(\theta) + v)^2}$ , the angle is  $\theta = \pi/3$ , the material parameter is  $A$ , and  $d = 2R$  is the particle diameter. The nonlinearity strength is controlled by the term  $\delta_0 > 0$ , which represents how much the granular packing is recompressed (see figure 10(b)). Unlike many 2D systems (such as photonic systems [3, 4]), one can compute the dispersion relation (see figure 11(b)) explicitly (using a 2D discrete Fourier transform) instead of relying on numerical computations [33].

In a hexagonal granular lattice, the dispersion surface has so-called ‘Dirac points’, at which upward-pointing and downward-pointing cones meet [78, 131]. A notable example of another physical system that possesses Dirac points is graphene (a monolayer of graphite that exhibits considerable electron mobility [152, 153]). One can thus consider a hexagonally packed granular crystal to be a ‘phononic’ analog of graphene; see also [11, 193, 194]. For wavenumbers near a Dirac point, one can derive so-called ‘Dirac equations’ as a continuum model using the methods described in this review [33]. The significance of this derivation is that ‘conical diffraction’ (where the dynamics have the form of an expanding ring, as illustrated in figure 11(c)) is possible in a Dirac system [5]. Numerical simulations of equation (41) validate the presence of conical diffraction in a hexagonal granular crystal when there are small-amplitude excitations. Studies of conical diffraction (or refraction) date back nearly two centuries [78, 131], and conical diffraction has also been studied at length (both theoretically and experimentally) in photonic graphene [3, 157]. The presence of nonlinearity can play a crucial role in conical-diffraction dynamics, and potentially it can even lead to a breakdown of conical wave propagation in honeycomb lattices [5, 14]. The preliminary numerical simulations of [33] illustrate that conical diffraction can break down for significantly nonlinear responses. The study of the effects of nonlinearity on conical diffraction through, for example, the derivation of a nonlinear Dirac system, is an open problem.

## 9. Conclusions and outlook

Granular crystals are an exciting mechanical metamaterial, and studying them brings together challenging problems from applied mathematics, scientific computation, condensed-matter and nonlinear physics (as well as other areas of physics), and experimental engineering. In this review, we have tried to illustrate the excitement that has been stimulated by recent advances in investigations of some of the prototypical nonlinear structures in granular crystals: solitary waves, dispersive shocks, and breathers.

A unifying theme of our review concerns approaches based on continuum approximations and asymptotics, which are illuminating in the study of all three families of structures. Although the continuum models provide important insights, they also suggest many open and nontrivial mathematical questions regarding their validity. (Even from a purely mathematical perspective, the equations themselves are intrinsically fascinating.) The numerical algorithms that are used for the identification of genuine traveling waves, and especially for stability computations, are at a very early stage. The algorithm that we described for the numerical computation of breathers is adequate for 1D granular crystals (i.e. granular chains), but it is too inefficient for 2D crystals, creating the need for new and faster algorithms, especially for large-scale computations of periodic orbits. The experimental realization of phenomena such as conical diffraction and structures such as 2D breathers remain open, and a particular challenge arises from the need to incorporate important additional dynamical features, such as torsion and rotation, that play stronger roles in 2D systems than in 1D systems. Throughout the review, we have also highlighted numerous other fascinating open issues. As we have discussed, granular crystals have an amazing amount of tunability: one can consider particles with different masses, sizes, material properties, and geometries; one can consider different particle configurations (monomer chains, dimer chains, other periodic chains, chains with defects, and random configurations in 1D, and an even larger variety of possibilities in 2D); and one can tune precompression to examine crystals in either weakly nonlinear regimes or strongly nonlinear regimes, where the latter is understood far more poorly than the former. All of these features, along with numerous prototypes for applications—involving sensing, lensing, gating, impact mitigation, vibration absorption, and more—render granular crystals an exciting test bed for the implementation of linear and nonlinear, theoretical and applied, mathematical, physical, and engineering concepts. The study of granular crystals promises to be an exciting area for many years to come.

## Acknowledgments

This material is based upon work supported by the National Science Foundation via grant number DMS-1615037. PGK gratefully acknowledges the support of the US Air Force Office of Scientific Research via grant number FA9550-12-1-0332 of the ERC under FP7; the Marie Curie Actions, People, International Research Staff Exchange Scheme (IRSES-605096); the ARO via grant number W911NF-15-1-0604; and the Alexander von Humboldt Foundation. CD acknowledges support from the U.S. Air Force Office of Scientific Research via grant number FA9550-12-1-0091.

## References

- [1] Abd-Elhady M S, Abd-Elhady S, Rindt C C M and van Steenhoven A A 2010 Force propagation speed in a bed of particles due to an incident particle impact *Adv. Powder Tech.* **21** 150

- [2] Ablowitz M J and Hoefler M 2009 Dispersive shock waves *Scholarpedia* **4** 5562
- [3] Ablowitz M J, Nixon S D and Zhu Y 2009 Conical diffraction in honeycomb lattices *Phys. Rev. A* **79** 053830
- [4] Ablowitz M J and Zhu Y 2010 Evolution of Bloch-mode-envelopes in two-dimensional generalized honeycomb lattices *Phys. Rev. A* **82** 013840
- [5] Ablowitz M J and Zhu Y 2013 Nonlinear dynamics of bloch wave packets in honeycomb lattices *Spontaneous Symmetry Breaking, Self-Trapping, and Josephson Oscillations* (Berlin: Springer) p 1
- [6] Achilleos V, Theocharis G and Skokos C 2016 Energy transport in one-dimensional disordered granular solids *Phys. Rev. E* **93** 022903
- [7] Ahnert K and Pikovsky A 2009 Compactons and chaos in strongly nonlinear lattices *Phys. Rev. E* **79** 026209
- [8] Allein F, Tournat V, Gusev V and Theocharis G 2016 Tunable magneto-granular phononic crystals *Appl. Phys. Lett.* **108** 161903
- [9] Anderson P W 1958 Absence of diffusion in certain random lattices *Phys. Rev.* **109** 1492
- [10] Anfosso J and Gibiat V 2004 Elastic wave propagation in a three-dimensional periodic granular medium *Europhys. Lett.* **67** 376
- [11] Antonakakis T, Craster R V and Guenneau S 2013 High-frequency homogenization of zero-frequency stop band photonic and phononic crystals *New J. Phys.* **15** 103014
- [12] Aubry S 2006 Discrete breathers: localization and transfer of energy in discrete Hamiltonian nonlinear systems *Physica D* **216** 1
- [13] Awasthi A P, Smith K J, Geubelle P H and Lambros J 2012 Propagation of solitary waves in 2D granular media: a numerical study *Mech. Mater.* **54** 100
- [14] Bahat-Treidel O, Peleg O, Segev M and Buljan H 2010 Breakdown of Dirac dynamics in honeycomb lattices due to nonlinear interactions *Phys. Rev. A* **82** 013830
- [15] Bardenhagen S G and Brackbill J U 1998 Dynamic stress bridging in granular materials *J. Appl. Phys.* **83** 5732
- [16] Behringer R P 2015 Jamming in granular materials *C. R. Phys.* **16** 10
- [17] Binder P, Abraimov D, Ustinov A V, Flach S and Zolotaryuk Y 2000 Observation of breathers in Josephson ladders *Phys. Rev. Lett.* **84** 745
- [18] Boechler N, Eliason J K, Kumar A, Maznev A A, Nelson K A and Fang N 2013 Interaction of a contact resonance of microspheres with surface acoustic waves *Phys. Rev. Lett.* **111** 036103
- [19] Boechler N, Theocharis G and Daraio C 2010 Bifurcation based acoustic switching and rectification *Nat. Mater.* **10** 665
- [20] Boechler N, Theocharis G, Job S, Kevrekidis P G, Porter M A and Daraio C 2010 Discrete breathers in one-dimensional diatomic granular crystals *Phys. Rev. Lett.* **104** 244302
- [21] Bonanomi L, Theocharis G and Daraio C 2015 Wave propagation in granular chains with local resonances *Phys. Rev. E* **91** 033208
- [22] Brandes T and Kettemann S 1993 *The Anderson Transition and its Ramifications—Localisation, Quantum Interference, and Interactions* (Berlin: Springer)
- [23] Brilliantov N V, Pimenova A V and Goldobin D S 2015 A dissipative force between colliding viscoelastic bodies: rigorous approach *Europhys. Lett.* **109** 14005
- [24] Burgoyne H and Daraio C 2014 Strain-rate-dependent model for the dynamic compression of elastoplastic spheres *Phys. Rev. E* **89** 032203
- [25] Burgoyne H A 2016 Dynamics of granular crystals with elastic–plastic contacts *PhD Dissertation* California Institute of Technology (<https://doi.org/10.7907/Z9J38QG6>)
- [26] Burgoyne H A and Daraio C 2015 Elastic–plastic wave propagation in uniform and periodic granular chains *J. Appl. Mech.* **82** 081002
- [27] Cabaret J, Béquin P, Theocharis G, Andreev V, Gusev V E and Tournat V 2015 Nonlinear hysteretic torsional waves *Phys. Rev. Lett.* **115** 054301
- [28] Campbell D K, Flach S and Kivshar Y S 2004 Localizing energy through nonlinearity and discreteness *Phys. Today* **57** 43
- [29] Carretero-González R, Khatri D, Porter M A, Kevrekidis P G and Daraio C 2009 Dissipative solitary waves in granular crystals *Phys. Rev. Lett.* **102** 024102
- [30] Charalampidis E G, Li F, Chong C, Yang J and Kevrekidis P G 2015 Time-periodic solutions of driven-damped trimer granular crystals *Math. Probl. Eng.* **2015** 830978
- [31] Chatterjee A 1999 Asymptotic solution for solitary waves in a chain of elastic spheres *Phys. Rev. E* **59** 5912
- [32] Chirilus-Bruckner M, Chong C, Prill O and Schneider G 2012 Rigorous description of macroscopic wave packets in infinite periodic chains of coupled oscillators by modulation equations *Discrete Continuous Dyn. Syst. S* **5** 879
- [33] Chong C, Kevrekidis P G, Ablowitz M J and Ma Y P 2016 Conical wave propagation and diffraction in 2D hexagonally packed granular lattices *Phys. Rev. E* **93** 012909
- [34] Chong C, Kevrekidis P G and Schneider G 2014 Justification of leading order quasicontinuum approximations of strongly nonlinear lattices *Discrete Continuous Dyn. Syst. A* **34** 3403
- [35] Chong C, Kevrekidis P G, Theocharis G and Daraio C 2013 Dark breathers in granular crystals *Phys. Rev. E* **87** 042202
- [36] Chong C, Kim E, Charalampidis E G, Kim H, Li F, Kevrekidis P G, Lydon J, Daraio C and Yang J 2016 Nonlinear vibrational-state excitation and piezoelectric energy conversion in harmonically driven granular chains *Phys. Rev. E* **93** 052203
- [37] Chong C, Li F, Yang J, Williams M O, Kevrekidis I G, Kevrekidis P G and Daraio C 2014 Damped-driven granular chains: an ideal playground for dark breathers and multibreathers *Phys. Rev. E* **89** 032924
- [38] Collins M A 1981 A quasicontinuum approximation for solitons in an atomic chain *Chem. Phys. Lett.* **77** 342
- [39] Coste C, Falcon E and Fauve S 1997 Solitary waves in a chain of beads under Hertz contact *Phys. Rev. E* **56** 6104
- [40] Coste C and Gilles B 1999 On the validity of Hertz contact law for granular material acoustics *Euro. Phys. J. B* **7** 155
- [41] Coste C and Gilles B 2008 Sound propagation in a constrained lattice of beads: High-frequency behavior and dispersion relation *Phys. Rev. E* **77** 021302
- [42] Cundall P A and Strack O D L 1979 A discrete numerical model for granular assemblies *Géotechnique* **29** 47
- [43] Bonanomi L 2012 *Locally Resonant Granular Crystals (Tesi di Laurea, Università degli Studi di Milano)* (<https://doi.org/10.1680/geot.1979.29.1.47>)
- [44] Daraio C and Nesterenko V F 2006 Strongly nonlinear waves in a chain of polymer coated steel beads *Phys. Rev. E* **73** 026612
- [45] Daraio C, Nesterenko V F, Herbold E B and Jin S 2006 Energy trapping and shock disintegration in a composite granular medium *Phys. Rev. Lett.* **96** 058002
- [46] Daraio C, Nesterenko V F and Jin S 2005 Strongly nonlinear waves in a chain of Teflon beads *Phys. Rev. E* **72** 016603
- [47] Daripa P and Hua W 1999 A numerical study of an ill-posed Boussinesq equation arising in water waves and nonlinear lattices: filtering and regularization techniques *Appl. Math. Comput.* **101** 159
- [48] Dauxois T 2008 Fermi, Pasta, Ulam, and a mysterious lady *Phys. Today* **61** 55

- [49] de Billy M 2001 Frequency analysis of the acoustic signal transmitted through a one-dimensional chain of metallic spheres *J. Acoust. Soc. Am.* **110** 710
- [50] Doney R and Sen S 2006 Decorated, tapered, and highly nonlinear granular chain *Phys. Rev. Lett.* **97** 155502
- [51] Doney R L, Agui J H and Sen S 2009 Energy partitioning and impulse dispersion in the decorated, tapered, strongly nonlinear granular alignment: a system with many potential applications *J. Appl. Phys.* **106** 064905
- [52] Drazin P G and Johnson R S 1989 *Solitons: an Introduction* (Cambridge: Cambridge University Press) (<https://doi.org/10.1002/qj.49711649114>)
- [53] Duanmu M, Whitaker N, Kevrekidis P G, Vainchtein A and Rubin J 2016 Traveling wave solutions in a chain of periodically forced couple nonlinear oscillators *Physica D* **325** 25
- [54] Dumas E and Pelinovsky D E 2014 Justification of the log-KdV equation in granular chains: the case of precompression *SIAM J. Math. Anal.* **46** 4075
- [55] English J M and Pego R L 2005 On the solitary wave pulse in a chain of beads *Proc. AMS* **133** 1763
- [56] English L Q, Sato M and Sievers A J 2003 Modulational instability of nonlinear spin waves in easy-axis antiferromagnetic chains. II. Influence of sample shape on intrinsic localized modes and dynamic spin defects *Phys. Rev. B* **67** 024403
- [57] Erofeev V I, Kazhaev V V and Pavlov I S 2013 *Nonlinear Localized Strain Waves in a 2D Medium with Microstructure* (Berlin: Springer) p 91
- [58] Falls W J and Sen S 2014 Solitary wave propagation through two-dimensional treelike structures *Phys. Rev. E* **89** 023209
- [59] Faver T E and Wright J D 2015 Exact diatomic Fermi–Pasta–Ulam–Tsingou solitary waves with optical band ripples at infinity (arXiv:1511.00942)
- [60] Fermi E, Pasta J and Ulam S 1955 Studies of nonlinear problems. I *Technical Report*, Los Alamos National Laboratory, Los Alamos, NM, USA LA–1940
- [61] Flach S 2015 Nonlinear lattice waves in random potentials *Nonlinear Optical and Atomic Systems (Lecture Notes in Mathematics* vol 2146) (Berlin: Springer) p 1
- [62] Flach S and Gorbach A 2008 Discrete breathers: advances in theory and applications *Phys. Rep.* **467** 1
- [63] Flach S and Gorbach A V 2005 Discrete breathers in Fermi–Pasta–Ulam lattices *Chaos* **15** 015112
- [64] Fraternali F, Porter M A and Daraio C 2010 Optimal design of composite granular protectors *Mech. Adv. Mat. Struct.* **17** 1
- [65] Friesecke G and Pego R L 1999 Solitary waves on Fermi–Pasta–Ulam lattices: II. Qualitative properties, renormalization and continuum limit *Nonlinearity* **12** 1601
- [66] Friesecke G and Pego R L 2002 Solitary waves on Fermi–Pasta–Ulam lattices: I. Linear implies nonlinear stability *Nonlinearity* **15** 1343
- [67] Friesecke G and Pego R L 2004 Solitary waves on Fermi–Pasta–Ulam lattices: III. Howland-type floquet theory *Nonlinearity* **17** 207
- [68] Friesecke G and Pego R L 2004 Solitary waves on Fermi–Pasta–Ulam lattices: IV. Proof of stability at low energy *Nonlinearity* **17** 229
- [69] Friesecke G and Wattis J A D 1994 Existence theorem for solitary waves on lattices *Commun. Math. Phys.* **161** 391
- [70] Gaison J, Moskow S, Wright J D and Zhang Q 2014 Approximation of polyatomic FPU lattices by KdV equations *Multiscale Model. Simul.* **12** 953
- [71] Gallavotti G 2008 *The Fermi–Pasta–Ulam Problem: a Status Report* (Berlin: Springer)
- [72] Gantzounis G, Serra-Garcia M, Homma K, Mendoza J M and Daraio C 2013 Granular metamaterials for vibration mitigation *J. Appl. Phys.* **114** 093514
- [73] Gilles B and Coste C 2003 Low-frequency behavior of beads constrained on a lattice *Phys. Rev. Lett.* **90** 174302
- [74] Glam B, Igra O, Britan A and Ben-Dor G 2007 Dynamics of stress wave propagation in a chain of photoelastic discs impacted by a planar shock wave; part I, experimental investigation *Shock Waves* **17** 1
- [75] Gómez-Gardeñes J, Falo F and Floría L M 2004 Mobile localization in nonlinear Schrödinger lattices *Phys. Lett. A* **332** 213
- [76] Gonzalez M, Yang J, Daraio C and Ortiz M 2012 Mesoscopic approach to granular crystal dynamics *Phys. Rev. E* **85** 016604
- [77] Hairer E, Nørsett S and Wanner G 1993 *Solving Ordinary Differential Equations I* (Berlin: Springer) (<https://doi.org/10.1007/978-3-540-78862-1>)
- [78] Hamilton W R 1837 Third supplement to an essay on the theory of systems of rays *Trans. R. Irish Acad.* **17** 1
- [79] Harbola U, Rosas A, Esposito M and Lindenberg K 2009 Pulse propagation in tapered granular chains: an analytic study *Phys. Rev. E* **80** 031303
- [80] Harbola U, Rosas A, Romero A H, Esposito M and Lindenberg K 2009 Pulse propagation in decorated granular chains: An analytical approach. *Phys. Rev. E* **80** 051302
- [81] Herbold E B and Nesterenko V F 2007 Shock wave structure in a strongly nonlinear lattice with viscous dissipation *Phys. Rev. E* **75** 021304
- [82] Herrmann M and Rademacher J D M 2010 Riemann solvers and undercompressive shocks of convex FPU chains *Nonlinearity* **23** 277
- [83] Hertz H 1881 Über die Berührung fester elastischer Körper *J. Reine Angew. Math.* **92** 156
- [84] Hochstrasser D, Mertens F and Büttner H 1989 An iterative method for the calculation of narrow solitary excitations on atomic chains *Physica D* **35** 259
- [85] Hong J 2005 Universal power-law decay of the impulse energy in granular protectors *Phys. Rev. Lett.* **94** 108001
- [86] Hoogeboom C and Kevrekidis P 2012 Breathers in periodic granular chains with multiple band gaps *Phys. Rev. E* **86** 061305
- [87] Hoogeboom C, Man Y, Boechler N, Theocharis G, Kevrekidis P G, Kevrekidis I G and Daraio C 2015 Hysteresis loops and multi-stability: from periodic orbits to chaotic dynamics (and back) in diatomic granular crystals *Europhys. Lett.* **101** 44003
- [88] Huang G and Hu B 1998 Asymmetric gap soliton modes in diatomic lattices with cubic and quartic nonlinearity *Phys. Rev. B* **57** 5746
- [89] Huang G, Shi Z P and Xu Z 1993 Asymmetric intrinsic localized modes in a homogeneous lattice with cubic and quartic anharmonicity *Phys. Rev. B* **47** 14561
- [90] James G 2003 Centre manifold reduction for quasilinear discrete systems *J. Nonlin. Sci.* **13** 27
- [91] James G 2011 Nonlinear waves in Newton’s cradle and the discrete p-Schrödinger equation *Math. Models Meth. Appl. Sci.* **21** 2335
- [92] James G, Kevrekidis P G and Cuevas J 2013 Breathers in oscillator chains with Hertzian interactions *Physica D* **251** 39
- [93] James G and Pelinovsky D 2014 Gaussian solitary waves and compactons in Fermi–Pasta–Ulam lattices with Hertzian potentials *Proc. R. Soc. A* **470** 20130462
- [94] James G and Starosvetsky Y 2014 Breather solutions of the discrete p-Schrödinger equation *Localized Excitations in Nonlinear Complex Systems (Nonlinear Systems and Complexity* vol 7) (Berlin: Springer) p 77
- [95] Jayaprakash K R, Starosvetsky Y and Vakakis A F 2011 New family of solitary waves in granular dimer chains with no precompression *Phys. Rev. E* **83** 036606

- [96] Jayaprakash K R, Starosvetsky Y, Vakakis A F and Gendelman O V 2013 Nonlinear resonances leading to strong pulse attenuation in granular dimer chains *J. Nonlinear Sci.* **23** 363
- [97] Job S and Melo F 2005 How Hertzian solitary waves interact with boundaries in a 1D granular medium *Phys. Rev. Lett.* **94** 178002
- [98] Job S, Santibanez F, Tapia F and Melo F 2008 Nonlinear waves in dry and wet Hertzian granular chains *Ultrasonics* **48** 506
- [99] Job S, Santibanez F, Tapia F and Melo F 2009 Wave localization in strongly nonlinear Hertzian chains with mass defect *Phys. Rev. E* **80** 025602
- [100] Johnson K L 1985 *Contact Mechanics* (Cambridge: Cambridge University Press)
- [101] Jones C K R T and Marangell R 2012 The spectrum of travelling wave solutions to the Sine-Gordon equation *Discrete Continuous Dyn. Sys. S* **5** 925
- [102] Kevrekidis P G, Cuevas-Maraver J and Pelinovsky D E 2016 Energy criterion for the spectral stability of discrete breathers *Phys. Rev. Lett.* **117** 094101
- [103] Kevrekidis P G, Frantzeskakis D J and Carretero-González R 2015 *The Defocusing Nonlinear Schrödinger Equation* (Philadelphia, PA: SIAM)
- [104] Kevrekidis P G, Kevrekidis I G, Bishop A R and Titi E S 2002 Continuum approach to discreteness *Phys. Rev. E* **65** 046613
- [105] Kevrekidis P G, Stefanov A G and Xu H 2016 Traveling waves for the mass in mass model of granular chains *Lett. Math. Phys.* **106** 1067
- [106] Kevrekidis P G, Vainchtein A, Serra-Garcia M and Daraio C 2013 Interaction of traveling waves with mass-with-mass defects within a Hertzian chain *Phys. Rev. E* **87** 042911
- [107] Khatri D, Daraio C and Rizzo P 2008 Highly nonlinear waves sensor technology for highway infrastructures in, nondestructive characterization for composite materials, aerospace engineering, civil infrastructure, and homeland security *Proc. SPIE* 6934 69340U
- [108] Khatri D, Ngo D and Daraio C 2012 Highly nonlinear solitary waves in chains of cylindrical particles *Granular Matter* **14** 63
- [109] Kim E, Chaunsali R, Xu H, Castillo J, Yang J, Kevrekidis P G and Vakakis A F 2015 Nonlinear low-to-high frequency energy cascades in diatomic granular crystals *Phys. Rev. E* **92** 062201
- [110] Kim E, Li F, Chong C, Theocharis G, Yang J and Kevrekidis P G 2015 Highly nonlinear wave propagation in elastic woodpile periodic structures *Phys. Rev. Lett.* **114** 118002
- [111] Kim E, Martínez A, Phenisee S, Kevrekidis P G, Porter M A and Yang J 2016 Direct measurement of superdiffusive energy transport and energy localization in disordered granular chains in preparation (arXiv:1705.08043)
- [112] Kim E and Yang J 2014 Wave propagation in single column woodpile phononic crystals: formation of tunable band gaps *J. Mech. Phys. Solids* **71** 33
- [113] Kittel C 2005 *Introduction to Solid State Physics* (New York: Wiley)
- [114] Lapyteva T V, Ivanchenko M V and Flach S 2015 Nonlinear lattice waves in heterogeneous media *J. Phys. A: Math. Theor.* **47** 493001
- [115] Lazarides N, Tsironis G P and Eleftheriou M 2008 Dissipative discrete breathers in rf SQUID metamaterials *Nonlinear Phen. Cplx. Syst.* **11** 250
- [116] Lazaridi A N and Nesterenko V F 1985 Observation of a new type of solitary waves in one-dimensional granular medium *J. Appl. Mech. Tech. Phys.* **26** 405
- [117] Lederer F, Stegeman G I, Christodoulides D N, Assanto G, Segev M and Silberberg Y 2008 Discrete solitons in optics *Phys. Rep.* **463** 1
- [118] Leonard A, Chong C, Kevrekidis P G and Daraio C 2014 Traveling waves in 2D hexagonal granular crystal lattices *Granular Matter* **16** 531
- [119] Leonard A and Daraio C 2012 Stress wave anisotropy in centered square highly nonlinear granular systems *Phys. Rev. Lett.* **108** 214301
- [120] Leonard A, Daraio C, Awasthi A and Geubelle P 2012 Effects of weak disorder on stress wave anisotropy in centered square nonlinear granular crystals *Phys. Rev. E* **86** 031305
- [121] Leonard A, Fraternali F and Daraio C 2013 Directional wave propagation in a highly nonlinear square packing of spheres *Exp. Mech.* **57** 327
- [122] Leonard A, Ponson L and Daraio C 2015 Exponential stress mitigation in structured granular composites *Extreme Mech. Lett.* **1** 23
- [123] LeVeque R J 1992 *Numerical Methods for Conservation Laws* (Basel: Birkhauser) (<https://doi.org/10.1007/978-3-0348-8629-1>)
- [124] Li F, Anzel P, Yang J, Kevrekidis P G and Daraio C 2014 Granular acoustic switches and logic elements *Nat. Commun.* **5** 5311
- [125] Li F, Zhao L, Tian Z, Yu L and Yang J 2013 Visualization of solitary waves via laser doppler vibrometry for heavy impurity identification in a granular chain *Smart Mater. Struct.* **22** 035016
- [126] Lin W and Daraio C 2016 Wave propagation in one-dimensional microscopic granular chains *Phys. Rev. E* **94** 052907
- [127] Lindenberg K, Harbola U, Romero A H and Rosas A 2011 Pulse propagation in granular chains *Int. Conf. on Applications in Nonlinear Dynamics—ICAND 2010 (AIP Conf. Proc. vol 1339)* (American Institute of Physics) p 97
- [128] Liu A and Nagel S R 2010 The jamming transition and the marginally jammed solid *Annu. Rev. Condens. Matter Phys.* **1** 347
- [129] Liu L, James G, Kevrekidis P and Vainchtein A 2016 Strongly nonlinear waves in locally resonant granular chains *Nonlinearity* **29** 3496
- [130] Liu L, James G, Kevrekidis P G and Vainchtein A 2016 Breathers in a locally resonant granular chain with precompression *Physica D* **331** 27
- [131] Lloyd H 1837 On the phenomena presented by light in its passage along the axes of biaxial crystals *Trans. R. Irish Acad.* **17** 145
- [132] Lydon J, Theocharis G and Daraio C 2015 Nonlinear resonances and energy transfer in finite granular chains *Phys. Rev. E* **91** 023208
- [133] MacKay R S 1999 Solitary waves in a chain of beads under Hertz contact *Phys. Lett. A* **251** 191
- [134] Makwana M and Craster R V 2013 Localised point defect states in asymptotic models of discrete lattices *Q. J. Mech. Appl. Math.* **66** 289
- [135] Man Y, Boechler N, Theocharis G, Kevrekidis P G and Daraio C 2012 Defect modes in one-dimensional granular crystals *Phys. Rev. E* **85** 037601
- [136] Martínez A J, Kevrekidis P G and Porter M A 2016 Superdiffusive transport and energy localization in disordered granular crystals *Phys. Rev. E* **93** 022902
- [137] Martínez A J, Yasuda H, Kim E, Kevrekidis P G, Porter M A and Yang J 2016 Scattering of waves by impurities in precompressed granular chains *Phys. Rev. E* **93** 052224
- [138] McDonald B E and Calvo D 2012 Simple waves in Hertzian chains *Phys. Rev. E* **85** 066602
- [139] Merkel A, Tournat V and Gusev V 2011 Experimental evidence of rotational elastic waves in granular phononic crystals *Phys. Rev. Lett.* **107** 225502
- [140] Molinari A and Daraio C 2009 Stationary shocks in periodic highly nonlinear granular chains *Phys. Rev. E* **80** 056602

- [141] Morsch O and Oberthaler M 2006 Dynamics of Bose–Einstein condensates in optical lattices *Rev. Mod. Phys.* **78** 179
- [142] Mueggenburg N W, Jaeger H M and Nagel S R 2002 Stress transmission through three-dimensional ordered granular arrays *Phys. Rev. E* **66** 031304
- [143] Mulder O M A W and Luding S 2006 Sound wave acceleration in granular materials *J. Stat. Mech.* P07023
- [144] Nayfeh A H and Mook D T 2004 *Nonlinear Oscillations* (New York: Wiley) (<https://doi.org/10.1002/9783527617586>)
- [145] Nesterenko V F 1983 Propagation of nonlinear compression pulses in granular media *J. Appl. Mech. Tech. Phys.* **24** 733
- [146] Nesterenko V F 2001 *Dynamics of Heterogeneous Materials* (New York: Springer) (<https://doi.org/10.1007/978-1-4757-3524-6>)
- [147] Nesterenko V F, Daraio C, Herbold E B and Jin S 2005 Anomalous wave reflection at the interface of two strongly nonlinear granular media *Phys. Rev. Lett.* **95** 158702
- [148] Ngo D, Khatri D and Daraio C 2011 Highly nonlinear solitary waves in chains of ellipsoidal particles *Phys. Rev. E* **84** 026610
- [149] Nguyen N S and Brogliato B 2014 *Multiple Impacts in Dissipative Granular Chains* (New York: Springer)
- [150] Nishida M and Tanaka Y 2010 DEM simulations and experiments for projectile impacting two-dimensional particle packings including dissimilar material layers *Granular Matter* **12** 357
- [151] Nishida M, Tanaka K and Ishida T 2009 DEM simulation of wave propagation in two-dimensional ordered array of particles *Shock Waves* (Berlin: Springer) p 815
- [152] Novoselov K S, Geim A K, Morozov S V, Jiang D, Katsnelson M I, Grigorieva I V, Dubonos S V and Firsov A A 2005 Two-dimensional gas of massless Dirac fermions in graphene *Nature* **438** 197
- [153] Novoselov K S, Geim A K, Morozov S V, Jiang D, Zhang Y, Dubonos S V, Grigorieva I V and Firsov A A 2004 Electric field effect in atomically thin carbon films *Science* **306** 666
- [154] On T, LaVigne P A and Lambros J 2014 Development of plastic nonlinear waves in one-dimensional ductile granular chains under impact loading *Mech. Mater.* **68** 29
- [155] On T, Wang E and Lambros J 2015 Plastic waves in one-dimensional heterogeneous granular chains under impact loading: single intruders and dimer chains *Int. J. Solids Struct.* **62** 81
- [156] Pal R K, Morton J, Wang E, Lambros J and Geubelle P H 2015 Impact response of elasto-plastic granular chains containing an intruder particle *J. Appl. Mech.* **73** 38
- [157] Peleg O, Bartal G, Freedman B, Manela O, Segev M and Christodoulides D N 2007 Conical diffraction and gap solitons in honeycomb photonic lattices *Phys. Rev. Lett.* **98** 103901
- [158] Peyrard M 2004 Nonlinear dynamics and statistical physics of DNA *Nonlinearity* **17** R1
- [159] Peyrard M and Daumont I 2002 Statistical properties of one-dimensional ‘turbulence’ *Europhys. Lett.* **59** 834
- [160] Ponson L, Boechler N, Lai Y M, Porter M A, Kevrekidis P G and Daraio C 2010 Nonlinear waves in disordered diatomic granular chains *Phys. Rev. E* **82** 021301
- [161] Porter M A, Daraio C, Herbold E B, Szelengowicz I and Kevrekidis P G 2008 Highly nonlinear solitary waves in periodic dimer granular chains *Phys. Rev. E* **77** 015601
- [162] Porter M A, Daraio C, Szelengowicz I, Herbold E B and Kevrekidis P G 2009 Highly nonlinear solitary waves in heterogeneous periodic granular media *Physica D* **238** 666
- [163] Porter M A, Kevrekidis P G and Daraio C 2015 Granular crystals: nonlinear dynamics meets materials engineering *Phys. Today* **68** 44
- [164] Pozharskiy D, Zhang Y, Williams M O, McFarland D M, Kevrekidis P G, Vakakis A F and Kevrekidis I G 2015 Nonlinear resonances and antiresonances of a forced sonic vacuum *Phys. Rev. E* **92** 063203
- [165] Roessig K M, Foster J C and Bardenhagen S G 2002 Dynamic stress chain formation in a two-dimensional particle bed *Exp. Mech.* **42** 329
- [166] Rosas A, Romero A H, Nesterenko V F and Lindenberg K 2007 Observation of two-wave structure in strongly nonlinear dissipative granular chains *Phys. Rev. Lett.* **98** 164301
- [167] Rosas A, Romero A H, Nesterenko V F and Lindenberg K 2008 Short-pulse dynamics in strongly nonlinear dissipative granular chains *Phys. Rev. E* **78** 051303
- [168] Rosenau P 1986 Dynamics of nonlinear mass-spring chains near the continuum limit *Phys. Lett. A* **118** 222
- [169] Rosenau P 2003 Hamiltonian dynamics of dense chains and lattices: or how to correct the continuum *Phys. Lett. A* **311** 39
- [170] Rosenau P and Hyman J M 1993 Compactons: solitons with finite wavelength *Phys. Rev. Lett.* **70** 564–7
- [171] Rucklidge A M and Silber M 2009 Design of parametrically forced patterns and quasipatterns *SIAM J. Appl. Dyn. Syst.* **8** 298
- [172] Sato M, Hubbard B E and Sievers A J 2006 *Colloquium: nonlinear energy localization and its manipulation in micromechanical oscillator arrays* *Rev. Mod. Phys.* **78** 137
- [173] Schneider G 2010 Bounds for the nonlinear Schrödinger approximation of the Fermi–Pasta–Ulam system *Appl. Anal.* **89** 1523
- [174] Schneider G and Wayne C E 2000 Counter-propagating waves on fluid surfaces and the continuum limit of the Fermi–Pasta–Ulam model *Proc. of Equadiff '99* vol 1 (Singapore: World Scientific) p 390
- [175] Schwarz U T, English L Q and Sievers A J 1999 Experimental generation and observation of intrinsic localized spin wave modes in an antiferromagnet *Phys. Rev. Lett.* **83** 223
- [176] Sen S, Hong J, Bang J, Avalos E and Doney R 2008 Solitary waves in the granular chain *Phys. Rep.* **462** 21
- [177] Shen Y, Kevrekidis P G, Sen S and Hoffman A 2014 Characterizing traveling-wave collisions in granular chains starting from integrable limits: the case of the Korteweg–de Vries equation and the Toda lattice *Phys. Rev. E* **90** 022905
- [178] Shukla A, Sadd M H, Xu Y and Tai Q M 1993 Influence of loading pulse duration on dynamic load transfer in a simulated granular medium *J. Mech. Phys. Solids* **41** 1795
- [179] Smoller J 1983 *Shock Waves and Reaction–Diffusion Equations* (Berlin: Springer)
- [180] Sokolow A and Sen S 2007 Exact solution to the problem of nonlinear pulse propagation through random layered media and its connection with number triangles *Ann. Phys.* **322** 2104
- [181] Spadoni A and Daraio C 2010 Generation and control of sound bullets with a nonlinear acoustic lens *Proc. Natl Acad. Sci. USA* **107** 7230
- [182] Starosvetsky Y, Hasan M A and Vakakis A F 2013 Nonlinear pulse equipartition in weakly coupled ordered granular chains with no precompression *J. Comput. Nonlinear Dyn.* **8** 034504
- [183] Starosvetsky Y and Vakakis A F 2010 Traveling waves and localized modes in one-dimensional homogeneous granular chains with no precompression *Phys. Rev. E* **82** 026603
- [184] Stefanov A and Kevrekidis P G 2012 On the existence of solitary traveling waves for generalized Hertzian chains *J. Nonlinear Sci.* **22** 327

- [185] Stefanov A and Kevrekidis P G 2013 Traveling waves for monomer chains with pre-compression *Nonlinearity* **26** 539
- [186] Swanson B I, Brozik J A, Love S P, Strouse G F, Shreve A P, Bishop A R, Wang W Z and Salkola M I 1999 Observation of intrinsically localized modes in a discrete low-dimensional material *Phys. Rev. Lett.* **82** 3288
- [187] Szelengowicz I, Hasan M A, Starosvetsky Y, Vakakis A and Daraio C 2013 Energy equipartition in two-dimensional granular systems with spherical intruders *Phys. Rev. E* **87** 032204
- [188] Szelengowicz I, Kevrekidis P G and Daraio C 2012 Wave propagation in square granular crystals with spherical interstitial intruders *Phys. Rev. E* **86** 061306
- [189] Theocharis G, Boechler N and Daraio C 2013 Nonlinear phononic periodic structures and granular crystals *Acoustic Metamaterials and Phononic Crystals* (Berlin: Springer) pp 217–51
- [190] Theocharis G, Boechler N, Kevrekidis P G, Job S, Porter M A and Daraio C 2010 Intrinsic energy localization through discrete gap breathers in one-dimensional diatomic granular crystals *Phys. Rev. E* **82** 056604
- [191] Theocharis G, Kavousanakis M, Kevrekidis P G, Daraio C, Porter M A and Kevrekidis I G 2009 Localized breathing modes in granular crystals with defects *Phys. Rev. E* **80** 066601
- [192] Topaz C M and Silber M 2002 Resonances and superlattice pattern stabilization in two-frequency forced Faraday waves *Physica D* **172** 1
- [193] Torrent D, Mayou D and Sánchez-Dehesa J 2013 Elastic analog of graphene: Dirac cones and edge states for flexural waves in thin plates *Phys. Rev. B* **87** 115143
- [194] Torrent D and Sánchez-Dehesa J 2012 Acoustic analogue of graphene: observation of Dirac cones in acoustic surface waves *Phys. Rev. Lett.* **108** 174301
- [195] Trías E, Mazo J J and Orlando T P 2000 Discrete breathers in nonlinear lattices: experimental detection in a Josephson array *Phys. Rev. Lett.* **84** 741
- [196] Turner C V and Rosales R R 1997 The small dispersion limit for a nonlinear semidiscrete system of equations *Stud. Appl. Math.* **99** 205
- [197] Vainchtein A, Starosvetsky Y, Wright J D and Perline R 2016 Solitary waves in diatomic chains *Phys. Rev. E* **93** 042210
- [198] Vakakis A F 2012 Analytical techniques for nonlinear periodic media *Wave Propagation in Linear and Nonlinear Periodic Media (International Center for Mechanical Sciences (CISM) Courses and Lectures)* (Berlin: Springer) p 257
- [199] Vergara L 2010 Model for dissipative highly nonlinear waves in dry granular systems *Phys. Rev. Lett.* **104** 118001
- [200] Wallis R F 1957 Effect of free ends on the vibration frequencies of one-dimensional lattices *Phys. Rev.* **105** 540
- [201] Wang S Y and Nesterenko V F 2015 Attenuation of short strongly nonlinear stress pulses in dissipative granular chains *Phys. Rev. E* **91** 062211
- [202] Wattis J A D 1993 Approximations to solitary waves on lattices. II. Quasi-continuum methods for fast and slow waves *J. Phys. A: Math. Gen.* **26** 1193
- [203] Xianglei N, Rizzo P and Daraio C 2011 Laser-based excitation of nonlinear solitary waves in a chain of beads *Phys. Rev. E* **84** 026601
- [204] Xu H, Kevrekidis P G and Stefanov A 2015 Traveling waves and their tails in locally resonant granular systems *J. Phys. A: Math. Theor.* **48** 195204
- [205] Xu J, Zheng B and Liu Y 2016 Solitary wave in one-dimensional buckyball system at nanoscale *Sci. Rep.* **6** 21052
- [206] Xu Y, Alexander T J, Sidhu H and Kevrekidis P G 2014 Instability dynamics and breather formation in a horizontally shaken pendulum chain *Phys. Rev. E* **90** 042921
- [207] Yang J, Dunatunga S and Daraio C 2012 Amplitude-dependent attenuation of compressive waves in curved granular crystals constrained by elastic guides *Acta Mech.* **223** 549
- [208] Yang J, Gonzalez M, Kim E, Agbasi C and Sutton M 2014 Attenuation of solitary waves and localization of breathers in 1D granular crystals visualized via high speed photography *Exp. Mech.* **54** 1043
- [209] Yang J and Sutton M 2015 Nonlinear wave propagation in a hexagonally packed granular channel under rotational dynamics *Int. J. Solids Struct.* **77** 65
- [210] Yasuda H, Chong C, Charalampidis E G, Kevrekidis P G and Yang J 2016 Formation of rarefaction waves in origami-based metamaterials *Phys. Rev. E* **93** 043004
- [211] Zabulionis D, Kačianauskas R, Markauskas D and Rojek J 2012 An investigation of nonlinear tangential contact behaviour of a spherical particle under varying loading *Bull. Pol. Acad. Sci. Tech. Sci.* **60** 265
- [212] Zabusky N J and Kruskal M D 1965 Interactions of solitons in a collisionless plasma and the recurrence of initial states *Phys. Rev. Lett.* **15** 240
- [213] Zabusky N J and Porter M A 2010 Soliton *Scholarpedia* **5** 2068
- [214] Zakharov V E and Shabat A B 1972 Exact theory of two-dimensional self-focusing and one-dimensional self-modulation of waves in nonlinear media *J. Exp. Theor. Phys.* **34** 62
- [215] Zhang Y, Pozharskiy D, McFarland D M, Kevrekidis P G, Kevrekidis I G and Vakakis A F 2015 Experimental study of nonlinear resonances and anti-resonances in a forced, ordered granular chain *Exp. Mech.* **57** 505
- [216] Zhao S 2007 On the spurious solutions in the high-order finite difference methods for eigenvalue problems *Comput. Methods Appl. Mech. Eng.* **196** 5031
- [217] Zhu Y, Shukla A and Sadd M H 1996 The effect of microstructural fabric on dynamic load transfer in two dimensional assemblies of elliptical particles *J. Mech. Phys. Sol.* **44** 1283